DURABILITY OF TERNARY BLENDED CEMENTS IN BRIDGE APPLICATIONS

A Thesis
presented to
the Faculty of the Graduate School
University of Missouri-Columbia

In Partial Fulfillment
of the Requirements for the Degree

Master of Science

---

by
CURTIS J. STUNDEBECK

Dr. V.S. Gopalaratnam, Thesis Supervisor

MAY 2007

The undersigned, appointed by the dean of the Graduate School, have examined the thesis entitled

DURABILITY OF TERNARY BLENDED
CEMENTS IN BRIDGE APPLICATIONS

presented by Curtis Stundebeck,
a candidate for the degree of master of science,
and hereby certify that, in their opinion, it is worthy of acceptance.

Professor V. S. Gopalaratnam

Professor Hani Salim

Professor Allen Thompson

ACKNOWLEDGEMENTS

The Portland Cement Association is gratefully acknowledged for their generous award of the PCA Research Fellowship. Without the financial support from this fellowship, I would not have been able to complete this project.

I would like to personally thank my thesis supervisor Dr. V. S. Gopalaratnam for his continuous guidance and support throughout the testing and completion of my thesis. A special thanks goes to the College of Engineering technicians. The knowledge of electronics and instrumentation by Mr. Richard Oberto are greatly appreciated. Construction of the RCPT testing apparatus would not have been possible without his assistance. Thanks also to Mr. Rick Wells for his assistance in machining the RCPT cells and the building of various other testing components.

Furthermore, I would like to extend my gratitude to a number of fellow graduate students. I would like to especially thank Mr. Patrick Earney for his help and input as we worked on this project together. Also deserving acknowledgement are Mr. Michael Ash, Mr. Ben Davis, Mr. John Meyer, Mr. Kenny DeYoung, and Mr. Wenqing Hu, who all provided great friendship and support throughout my career as a graduate student.

I would like to thank my parents, Bernie and Lois Stundebeck, and my brothers, Clint, Cliff, and Casey, for their constant encouragement and support as I completed my long career as a student at the University of Missouri-Columbia. Also deserving a tremendous word of gratitude is my fiancée, Lisa, for her continuous patience, encouragement, and proof-reading support as I completed my thesis. Finally, I would like to thank God for providing guidance and direction throughout the entire project.

TABLE OF CONTENTS

LIST OF FIGURES

PAGE

LIST OF TABLES

PAGE

DURABILITY OF TERNARY BLENDED CEMENTS IN BRIDGE APPLICATIONS

Curtis Stundebeck

Dr. V.S. Gopalaratnam, Thesis Supervisor

ABSTRACT

The long-term performance of bridge components can be greatly influenced by the durability parameters including freeze-thaw and chloride permeability resistance. Both freeze-thaw resistance and chloride permeability resistance were tested along with the compressive strength of 24 high performance concrete (HPC) mixtures. The effects of binary and ternary blended HPC including silica fume and fly ash were tested with respect to freeze thaw resistance and chloride permeability. The study included observations of how water to binder ratio and curing time affected the pore structure development of fly ash and silica fume concretes when tested using the Rapid Choride Permeability Test.

The chloride permeability test results prove that both fly ash and silica fume are useful in reduction of chloride permeability. It is evident that fly ash is generally much slower reacting than silica fume from the tests conducted at 7, 28, and 56 days of moist curing. Results also indicate an increase in chloride penetration with increased w/b ratio dependent upon cement composition. A reduction in chloride permeability values can also be seen with increased curing time with the largest reduction between 7 and 28 days when tests were conducted at 7, 28, and 56 days. The results indicate that properly air entrained HPC is generally resistant to the effects of freezing and thawing as there was minimal degradation of the dynamic modulus of elasticity in all specimens tested.

CHAPTER 1 INTRODUCTION

1.1 Project Motivation and Significance

The use of high performance concrete in the construction of highway bridges has become more important in recent years. Using high performance concrete (HPC) has the potential to lower both initial and life-cycle costs of bridges. Over the life of a bridge, improved serviceability performance achieved with the use of HPC can reduce maintenance and repair costs and increase the life of the structure. Durability issues that often degrade the performance of bridge structures are freeze-thaw damage and chloride permeability. Chlorides from roadway de-icing salts penetrate into the concrete and can be detrimental to the reinforcing steel in bridge decks. Other concrete serviceability issues that can be improved by the use of specially engineered cement blends are time dependent characteristics such as creep and shrinkage. In addition, the higher strength generally produced by HPC allows for longer girder spans and larger girder spacing, thus decreasing the number of girder lines and interior bents. This most often results in a reduction in initial bridge costs. The properties related to increased strength in HPC are generally well understood in the literature. However, there appears to be less of an understanding of the durability and time dependent properties of HPC in the available literature.

In addition to the enhanced performance of HPC, there are environmental advantages due to the use of industrial process byproducts. Both fly ash and silica fume are byproducts that must normally be disposed of with some cost and environmental risk. These risks are greatly reduced by using them in concrete. Concrete using fly ash can

actually be more economical than standard Portland cement concrete due to its availability and low cost.

1.2 Objective of the Research

The project was designed to develop a material level optimization of ternary blended high performance concrete for use in bridge applications. Such applications include the construction of girders, decks, columns, and foundations. The overall project included both time dependent performance properties such as creep and shrinkage as well as durability issues including chloride permeability and freeze-thaw resistance. The focus of the study included in this report is on the effect of pore structure and its development on durability issues tested on laboratory specimens.

This project involved measuring the chloride permeability and freeze-thaw resistance of 24 different high performance concrete mixes. This allowed for testing the performance of varying water to binder ratios and cement compositions. The effect of curing time of the specimens was also tested on chloride permeability resistance. These tests were conducted to develop an understanding of the microstructure effects and physical phenomenon behind chloride penetration and freeze-thaw resistance of high performance concrete. This study is unique as it provides a systematic variation of cement composition, water to binder ratios, and curing time having single variable for each test.

1.3 Thesis Organization

Chapter Two includes a literature review of the use of ternary blended HPC for bridge applications, describes tests used to measure durability, and explores the effects of

several parameters on the chloride permeability and freeze-thaw resistance. Chapter Three details the experimental program selected and the variables that were investigated in this study of high performance concrete. Chapter Four explains the test equipment and procedures used in conducting this study of HPC durability. Chapter Five provides plots of compressive strength, freeze-thaw, and chloride permeability results and discusses these results in detail. Chapter Six provides a summary of the project and conclusions drawn from the test results.

CHAPTER 2 LITERATURE REVIEW

2.1 Ternary Blend HPC for Bridge Applications

Durability issues, including freeze thaw and chloride permeability resistance, can greatly influence the long-term performance of bridges. The reduction in costs associated with the use of supplementary cementitious materials is also significant in reducing initial bridge costs. Fly ash is a by-product of coal combustion in power plants; therefore, its use in concrete provides an environmentally friendly solution to disposal. Blomberg (2003) reported costs of fly ash, silica fume, and Portland cement as $22, $800, and $83 per ton, respectively. The availability and lower cost for fly ash indicate that it could be an economical replacement for Portland cement in suitable applications. Silica fume, being relatively expensive in comparison to Portland cement, can still be used effectively to provide desirable durability and other physical characteristics that would not be possible with Portland cement only. Silica fume is rarely used as more than a 10% cement replacement. This increase for silica fume concrete is generally offset by reduced maintenance and repair costs and reduced initial costs from the resulting higher strength concrete.

2.1.1 Pore Structure Difference

Reduced chloride permeability results from a finer pore structure and a smaller amount of calcium hydroxide in the hardened paste. Permeability is generally governed by the pore structure in concrete rather than the porosity. Porous concretes can have a low permeability if the pores are not connected (Chia and Zhang 2002). In the hydration process of Portland cement, large capillary pores are filled with hydration products,

decreasing the size of the large pores and increasing the volume of fine gel pores. Supplementary cementitious materials react with calcium hydroxide formed in the hydration process of the Portland cement. This allows an even further refining of the concrete's pore structure, as products of this secondary reaction are added to the hardened paste. The volume previously taken by calcium hydroxide is also filled in. This reduction in pore size is the main reason for concrete's increased resistance to permeability with the use of fly ash, silica fume, and ground granulated blast furnace slag (Hooton 1986).

2.1.2 Bridge Component Requirements

In the process of optimizing high performance concrete mixtures for highway bridge applications, it is important to understand that various bridge components require different physical and mechanical properties. In pre-stressed concrete I-girders, strength, stiffness, creep, and shrinkage properties are more important than durability since they are protected from direct exposure to water and de-icing salts. Higher strength and stiffness can lead to longer spans and larger girder spacing. Reduction in time dependent effects, including both creep and shrinkage, are significant in minimizing long-term pre-stressing loss and stresses created at girder ends. Concrete bridge decks and foundations, on the other hand, generally require lower strength and stiffness, but increased resistance to freeze-thaw and chloride penetration is essential in areas where the possibility of exposure to de-icing salts and ponded water in freezing temperatures is more prevalent. It is necessary to optimize concrete mixtures with respect to its application in various different bridge components.

2.2 Chloride Penetration

Resistance to chloride permeability is an important issue in the optimization of concrete mixtures to be used in bridge decks. A number of variables exist in concrete's mix design and curing regime that can affect its chloride penetration resistance. Chloride ions penetrate concrete by a number of different mechanisms, including capillary absorption, hydrostatic pressure, and diffusion. Diffusion, the most common method of chloride ion movement, requires a continuous liquid phase and a chloride ion concentration gradient. The second means for chloride ingression is permeation due to an applied hydraulic head with chlorides present on the concrete surface. Absorption, also a common method for chloride transport, involves water potentially containing chlorides to be drawn into the pore structure through capillary suction. This method is driven by moisture gradients and will generally not independently bring chlorides to the level of the reinforcing steel, unless the concrete quality is poor or the steel is very shallow (Stanish et al. 1997).

2.2.1 Testing Methods

There are standard tests prescribed for measuring the permeability of chloride into concrete. Three common tests are the Rapid Chloride Penetration Test, 90-day Chloride Ponding Test, and the Rapid Migration Test. Many researchers have modified the standard tests to better suit permeability testing of high performance concrete.

The Standard Method of Test for Resistance of Concrete to Chloride Penetration (AASHTO T 259 2001), commonly known as the Chloride Ponding Test, is the oldest test for measuring chloride ion penetration. Three inch thick by 12 inch square slabs are cast and moist cured for 14 days and stored in a drying room until 28 days of age. A dam

approximately ¾-inch tall is placed around the perimeter of the slab. Following an additional 13 days in the drying room, the slabs are subjected to a 90 day continuous ponding with ½-inch of 3% sodium chloride solution as shown in Figure 2-1. Samples of the specimen are taken using a grinding procedure from 1/16-inch to ½-inch and ½-inch to 1-inch. The chloride contents of the samples are then determined with chemical titration process defined by (AASHTO T 260 2001). Companion specimens are cast and not subjected to the chloride ponding to determine the baseline chloride content in the specimens.

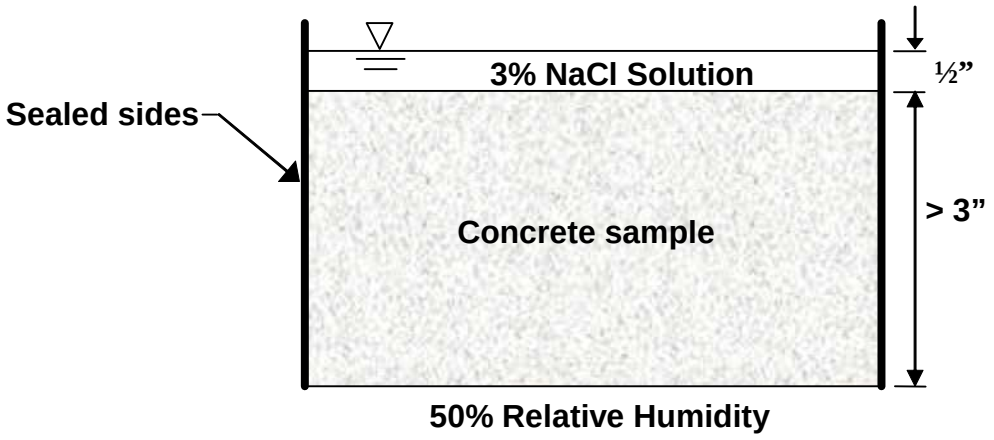

Figure 2-1: AASHTO T-259 salt ponding setup (Stanish et al. 1997)

A number of criticisms of the ponding test have been stated in the literature. The 90 day time for ponding is often criticized, especially since this time period may not allow for high quality concretes to develop a sufficient chloride penetration profile. Another problem with the test is it does not distinguish different chloride penetration mechanisms. The period of 28 days of drying prior to the beginning of the test allows for absorption when the specimen is initially subjected to the chloride solution. The fact that the bottom surface is exposed to 50% relative humidity also introduces the concept of wicking of the chloride solution from the wet surface toward the drier bottom face, due to

the large relative humidity gradient. These allow for chloride to be drawn into the concrete by mechanisms other than pure diffusion. There are also arguments that grinding ½" layers does not provide enough resolution to accurately see the chloride profile (Stanish et al. 1997).

To overcome some deficiencies of the ponding test, the bulk diffusion test (NordTest NTBuild 443) has been developed to measure chloride diffusion. To eliminate initial absorption effects, the specimens are saturated in limewater rather than allowing them to dry for 28 days prior to the test (Stanish et al. 1997).

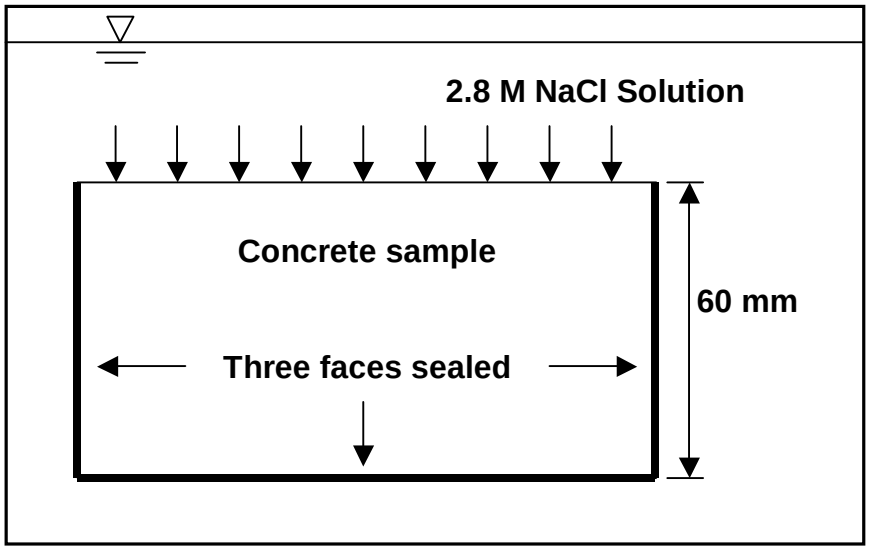

Figure 2-2: Nordtest setup (Stanish et al. 1997)

The Rapid Chloride Penetration Test, detailed in (American Society for Testing And Materials 1997b) and AASHTO T-277, was utilized in this project. The test monitors the electrical current during a 6-hour period that passes through a saturated 2-inch slice from the middle of a 4-inch diameter cylinder or core. One end of the specimen is immersed in a sodium chloride solution, and the other end is immersed in a sodium hydroxide solution as shown in Figure 2-3. A potential difference of 60 Volts is

applied to the ends of the specimen. Electrical current passing through the specimen is measured over a six-hour period. The area under the time-current plot is equivalent to the charge passed in Coulombs, an indication of the resistance of the concrete specimen to chloride penetration. The entire procedure and setup of the Rapid Chloride Penetration Test is discussed in greater detail in Chapter 4.

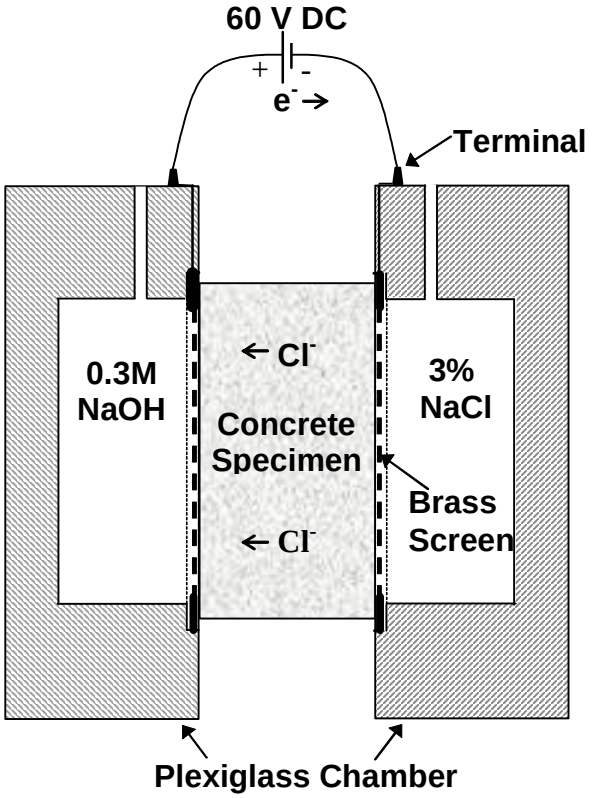

Figure 2-3: Rapid chloride permeability test setup

The Rapid Migration Test, first developed by Tang and Nilsson (1997) is defined in AASHTO TP 64-03 (2003). The test is similar to the RCPT, having a 2" thick and 4" diameter specimen subjected to an electrical potential to accelerate the chloride ion movement through a concrete specimen. The test setup used to conduct the Rapid migration test is shown in Figure 2-4. The bottom of the specimen is subjected to 10% sodium chloride solution, while a 0.3N sodium hydroxide solution is ponded on the top.

A 60V potential difference is initially applied across the specimen, and depending on the initial current, the voltage is lowered to 30 or 10 volts for more permeable concretes. After the test runs for 18 hours, the specimens are split longitudinally in two pieces and sprayed with 0.1 M silver nitrate solution to determine the chloride penetration depth profile. The rate of penetration is determined by dividing the penetration depth by the product of applied voltage and test duration.

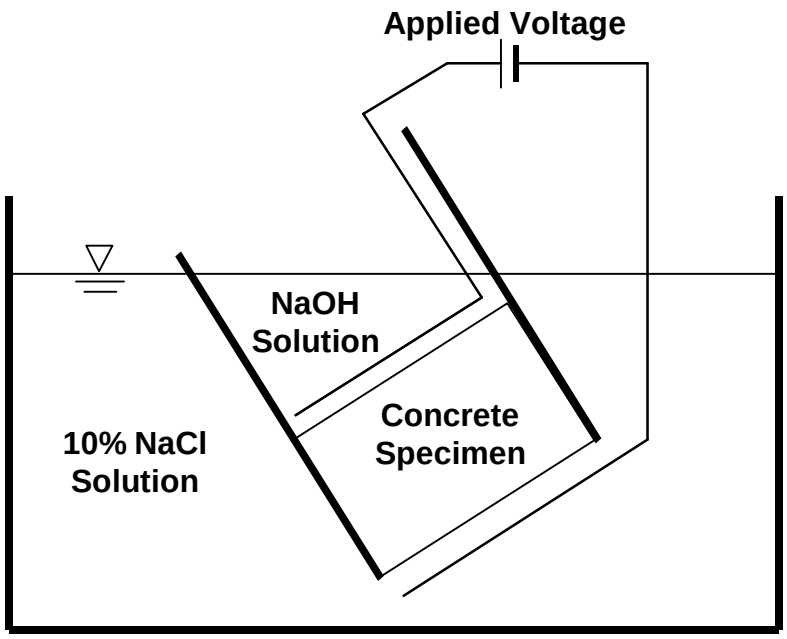

Figure 2-4: Rapid migration test setup

2.2.2 Effects of Cement Composition

The use of silica fume is well known to reduce chloride penetration. Silica fume is made up of very fine spherical particles generally consisting of at least 85% SiO2. The particle diameter averages about 0.1 μm, which is about 1/100 of the size of a typical Portland cement particle. When mixed with Portland cement, the silica fume quickly forms calcium silicate hydrate, resulting in a dense and relatively impermeable material

as the hydrate fills in normally weak spaces between the cement paste and aggregate particles.

In tests performed by (Oh et al. 2002) the chloride permeability of mixtures with water to binder ratios of 0.28 and 0.43 was observed. Silica fume had the greatest effect on reduction of chloride permeability compared to fly ash and slag. Silica fume mixes had chloride permeability values in the negligible range defined by ASTM C-1202, but cement replacement by silica fume of greater than 10% provided negligible effect to chloride permeability. The chloride permeability of mixtures with a 15% fly ash replacement level is about half compared to the control mixture.

Ozyildirim (1987) found that cement replacement by 5% silica fume in mixes with a w/b ratio of 0.35 and 0.4 the chloride permeability was reduced by a factor of 3-4. The tests were conducted using the RCPT after 56 days with two weeks of moist curing. The AASHTO Ponding test was also performed along with the RCPT tests. Mixes with silica fume had a chloride content in the ¼" to ¾" depth, about one half that of the control mix.

Plante and Bilodeau (1989) also observed that the addition of 8% silica fume to concrete mixtures reduced the charge passed in the RCPT by a factor 4-6 after 28 days of moist curing depending on the w/b ratio. The value of the reduction in chloride permeability was greater for the higher w/b ratio concretes.

Chia and Zhang (2002) conducted permeability tests on light-weight aggregate concrete and normal weight concrete with and without silica fume. Cement replacement by 10% silica fume in these mixtures reduced the chloride permeability by 5-6 times when tested by the RCPT. Results were similar from the ponding test and an immersion

test, where the chloride permeability depth was measured from the side casting surface of specimens split parallel to the top and bottom surface. With the addition of silica fume the chloride permeability depth was reduced to about half that of the control specimens with both light weight and normal weight concrete. The use of an expanded clay type aggregate in the lightweight concrete rather than crushed granite in the normal weight concrete had relatively no affect on the chloride permeability.

Luther and Mikols (1992) performed tests using the RCPT and found that concrete mixtures with less than 5% replacement of cement with silica fume had a chloride permeability in the very low range defined by ASTM. Addition of 34% slag replacement of cement reduced the total charge passed using the RCPT by more than 200 Coulombs.

Using the 90-day ponding test and a test similar to the RCPT but having only a 40V power supply, (Cabrera and Claisse 1990) found that the 20% replacement of cement with silica fume greatly reduced the chloride permeability. After 28 days of curing, the charge passed according to ASTM was in the very low or negligible range for the silica fume mixes but in the moderate range for the OPC mixes.

Babu (2001) showed that increased slag replacement and increased strength provides increased resistance to chloride permeability. The slag replacement level only had a significant effect on the mixtures with a design strength of 30 and 60 MPa. With mixtures having a compressive strength 80 to 90 MPa at 90 days and a water-binder ratio less than 0.3, the addition of slag had little effect on the chloride permeability resistance since it was near the ASTM low range without slag.

In tests conducted by the Hooton group at the University of Toronto in 1998, the chloride permeability of concretes with binary and ternary blended cements was tested using the Rapid Chloride Permeability Test. All mixes that included either slag or silica fume had low permeability according to ASTM with the exception of a mixture with 35% slag at 28 days curing as shown in Figure 2-5. In a concrete mixture with 8% silica fume, there appeared to be a slight increase in chloride permeability with curing time, but the addition of slag decreased this effect. A mixture having 5.2% silica fume and 35% slag by weight of total cement had the best chloride permeability performance having less than 300 Coulombs passing at all curing times tested. The ternary mixes performed better than all other mixes with regard to durability as suggested by Figure 2-5 (Bleszynski et al. 2002).

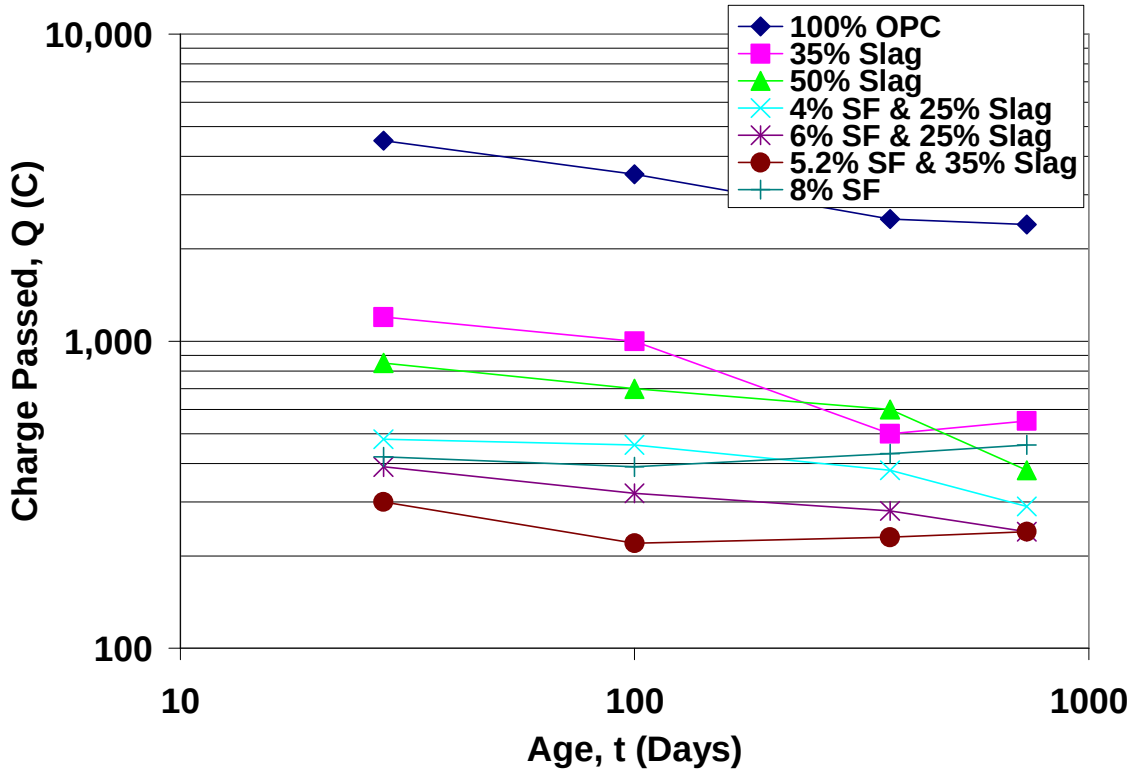

Figure 2-5: Influence of age on chloride permeability for control, binary, and ternary mixtures. Data from: (Bleszynski et al. 2002)

2.2.3 Effects of Water to Binder Ratio

The porosity of concrete is widely known to increase with increased water to binder ratio. More porous concrete allows for easier diffusion of chlorides and therefore larger values for permeability.

Ozyildirim (1987) observed that reducing the w/b ratio from 0.40 to 0.35 reduced the chloride permeability 60-70% when tested using the RCPT. The difference was more evident in the control mixes having no silica fume than mixes with 5% silica fume as the values for the mixtures containing silica fume were about one-third those of the control mixtures.

A noticeable reduction in chloride permeability in silica fume mixtures was observed by Plante and Bilodeau (1989) as the w/b ratios decreased from 0.66 to 0.21. The chloride permeability was related to the reduction in total porosity resulting from lower water to binder ratios.

Tests performed using the RCPT resulted in decreased permeability by a factor of approximately 5 with decreased w/b ratio from 0.43 to 0.28 (Oh et al. 2002). Values were in the “very low” or “negligible” range for chloride permeability defined by ASTM C-1202.

2.2.4 Effects of Curing Time

It appears that there are varying effects of curing time based on cement composition and water to binder ratio. In a study conducted by Blomberg (2003) at the Missouri Department of Transportation-Research, Development, Technology, 11 mixes designed for use on bridge decks were studied. The mixtures included control mixtures and binary and ternary HPC mixes containing fly ash, silica fume, and ground granulated

blast furnace slag. Most of the mixtures had a decrease in chloride permeability from 28 to 56 days of curing time that ranged from 25 to 45% as measured using the RCPT. The decrease was less significant from 56 to 90 days. The fly ash mixtures had further reductions in chloride permeability values of 20 to 30%, while silica fume and slag mixtures saw negligible chloride permeability reduction between 56 and 90 days.

A decrease in chloride permeability is evident with increased curing time from 1-7 and 7-28 days in silica fume mixes tested by Plante and Bilodeau (1989). The effect of reduction from increased curing time was also more evident in the concretes having higher w/b ratios. The chloride permeability was proportional to the porosity, which also was reduced with curing time.

Cabrera and Claisse (1990) also found a reduction in chloride permeability with the increased curing time. Control mixtures and mixtures with 20% silica fume, cured at 20°C and 100% relative humidity, were tested using a test similar to the RCPT having only 40V. The curing time had the greatest effect on a silica fume mix with a w/b ratio of 0.46. The charge passed decreased from over 6,000 Coulombs to about 500 Coulombs when tested at 3 and 28 days, respectively. The decrease from 28 to 90 days was around 200 Coulombs. A silica fume mix with a w/b ratio had similar results at 28 and 90 days, but at 3 days, the charge passed was only about 2,000 Coulombs.

Bleszynski et al.(2002) showed that curing time was important in the reduction of chloride permeability as seen in Figure 2-5. Chloride permeability was measured on the different mixes at 28, 100, 365, and 728 days. The reduction in permeability was reduced by the largest amount between 28 and 100 days.

2.3 Freeze Thaw

Significant damage caused by freeze-thaw resistance can generally be avoided with the use of quality aggregates, low water to cement ratio, proper air entrainment, and adequate curing before exposure to freeze-thaw cycles (ACI Committee 201 2001). Many investigations have indicated that HPC has a lower total porosity than normal concretes. The temperature at which water freezes in the capillary pores is dependent on the size of the pores. Water in 10 nm pores will freeze at -5˚C, however, water in 3.5 nm pores will not freeze until the temperature reaches -20˚C. As water freezes in saturated concrete, ice forms in the capillary pores, causing the remaining water to be compressed and create a hydraulic pressure. As additional pore water progressively freezes with lowering temperatures, the pressure increases, unless the water can escape to unfrozen pores with lower pressure. If the water does not escape, the capillaries expand, causing internal stresses and micro cracking in the concrete (Zia et al. 1991).

ASTM C-666 is used to determine the resistance of concrete to rapid freezing and thawing cycles. The specimens used for test prisms or cylinders are between 3 and 5 inches in width, depth or diameter and between 11 and 16 inches in length. Before the freeze-thaw test begins, the specimens are cured for 14 days unless otherwise specified for the testing of curing time effects. Before the test begins the weight and the fundamental transverse frequency of each specimen are measured. The fundamental transverse frequency is measured in order to calculate the dynamic modulus of elasticity. Specimens are inserted into metal containers filled with water to be placed in the freezing and thawing chamber. The temperature in the chamber cycles from 40°F ± 3°F to 0°F ± 3°F and back to 40°F ± 3°F in a time period between 2 and 5 hours. The test has two

different procedures that can be used. In Procedure A, the specimens are surrounded by water in both the freezing and the thawing cycles. In Procedure B the specimens are surrounded by air during the freezing phase and surrounded by water in the thawing phase. The fundamental transverse frequency of each specimen is measured when thawed at no more than every 36 cycles. The freeze-thaw test is stopped after 300 cycles or when the relative dynamic modulus reaches 60% of the initial value. The durability factor can then be calculated from the following equation.

$$DF = \frac{PN}{M} \qquad \text{Eq. (2.1)}$$

DF = Durability Factor

P = Relative Dynamic Modulus at N cycles expressed as a percentage

N = The least value of the number of cycles when P reaches a minimum value for terminating the test or the number of cycles for terminating the test

M = Specified number of cycles when the test is to be terminated

(American Society for Testing And Materials 1997a)

2.3.1 Effects of Air Entrainment

Entrained air in concrete provides space in the paste for excess capillary water to escape and freeze without causing severe damage. ACI Committee 201 (2001) recommends air contents of 3 to 7.5%, depending on the maximum aggregate size and exposure condition. Concrete without proper air entrainment will not be properly protected from freeze-thaw resistance; however, air entrainment beyond what is needed will cause a sacrifice in compressive strength. Entrained air provides empty space in the paste for excess capillary water to escape and freeze without causing damage to the

concrete. There are a number of articles that address the issue of whether air entrainment is needed for the freeze-thaw resistance of high performance concrete.

For mixes with a total cementitious materials content of at least 822 lb/ft^3 and a w/b ratio less than 0.28 the presence of entrained air increased the durability to at least 95 (Kashi and Weyers 1989). The durability factor at 300 cycles seems largely dependent upon the air content for mixtures with 19% Class C Fly Ash. All mixtures had a Durability Factor greater than 90 except for those with less than 3% air entrainment (Cramer 2001). For mixes with a w/b ratio of 0.33, mixes with and without silica fume failed the ASTM C-666 test having a relative dynamic modulus less than 0.6 after 300 cycles, air-entrained mixes all had relative dynamic modulus greater than 0.90 (Cohen et al. 1992).

In tests conducted prior to 1994 by Ghosh and Nasser, concrete mixtures with ternary blended cement having 10% silica fume and 20% fly ash and a w/b ratio of 0.27, the addition of air entrainment raised the durability factor only from 64 to 68 and 70 with with 4% and 8% air, respectively. With higher levels of fly ash, the addition of air entrainment was not advantageous in increasing the freeze-thaw durability (Ghosh and Nasser 1995). In tests conducted by Cohen, Zhou, and Dolch (1992) when properly air entrained there did not seem to be any effect positive or negative with the addition of 9% silica fume.

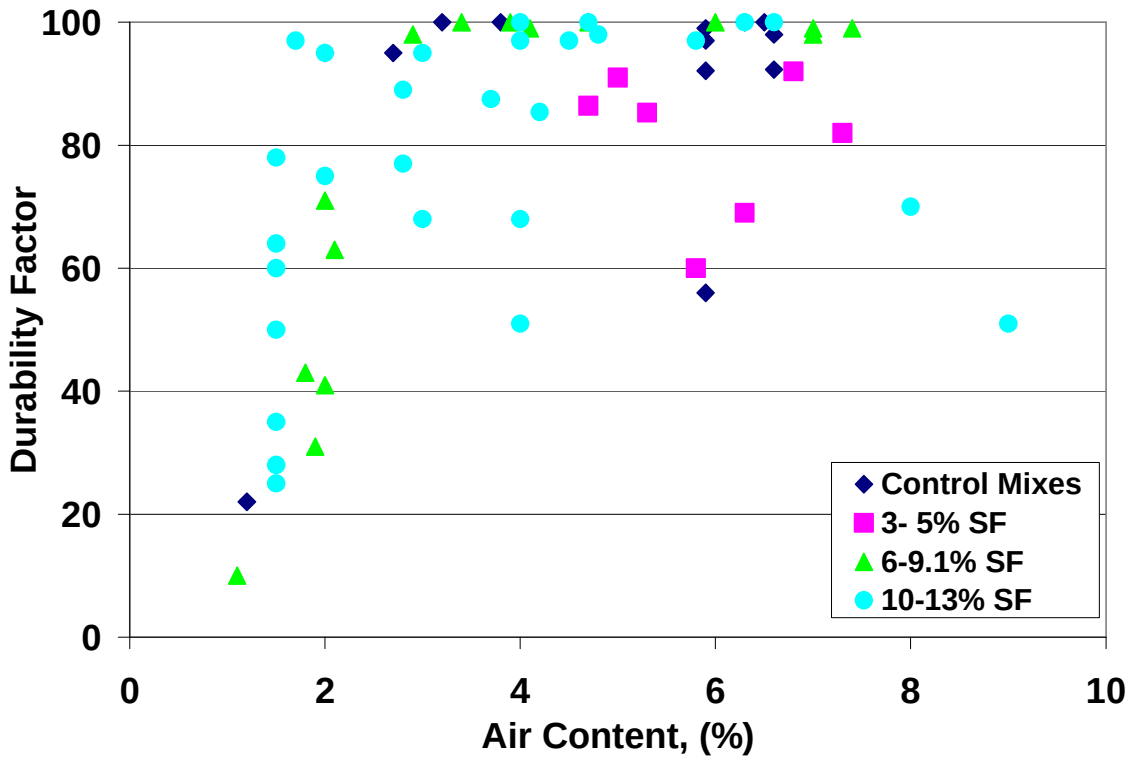

Figure 2-6: Effects of air entrainment on the freeze-thaw resistance of silica fume HPC and control mixtures. Data from: (Cohen et al. 1992);(Malhotra 1990);(Zia and Hansen 1993);(Ozyildirim 1987);(Kashi and Weyers 1989); (Ghosh and Nasser 1995)

Figure 2-6 includes a plot of the durability factor of air-entrained control and silica fume HPC mixtures. As long as air-entrainment is greater than 3%, silica fume HPC mixtures containing 5% silica fume as cement replacement exhibit good resistance to freeze-thaw per ASTM C 666. Higher additions of silica fume (beyond 5% cement replacement) do not significantly enhance the freeze-thaw resistance of air-entrained concrete. However, it would still be safer to ensure 3-4% entrained-air in all silica fume HPC mixtures with the use of an air entraining admixture. The marginal loss in strength due to this nominal air-entrainment is more than offset by the benefits of guaranteed freeze-thaw durability.

2.3.2 Effects of Cement Composition

Cramer (2001) investigated 12 different fly ash mixtures with a w/b ratio less than or equal to 0.45 and reported that the durability factor was 94 with or without 19% fly ash. This suggests that, like for silica fume HPC, as long as there is a nominal air-entrainment of 3%, the supplementary cementitious materials only contribute marginally to improved durability. Cramer also reports of similar observations with a slag HPC mixture (50% cement replacement), although he notes that the slag mixtures are more susceptible to surface damage and weight loss than similar mixtures made with 19% fly ash.

The replacement of cement with silica fume seems to have different effects on the freeze-thaw durability of concrete. For mixes with a relatively low water to binder ratio, there is a positive effect on concrete's durability as silica fume creates more pores which are small enough that water does not freeze in them at temperatures higher than -20°C. This provides the possibility of producing concrete that is freeze-thaw resistant without using entrained air (Zia et al. 1991). Hooton performed freeze-thaw tests between 1983 and 1990 on non air-entrained concrete with a w/(cement + silica fume) ratio of 0.35 and silica fume content ranging from 0 to 20%. The durability factor increased from 11.5 for the control specimen, which failed the 60% of original dynamic modulus criteria at only 58 cycles to durability factors above 90 at 300 cycles for the silica fume mixes. These silica fume mixtures survived 900 cycles with durability factors still above 90 (Hooton 1993). For properly air-entrained mixes, there doesn't seem to be a significant increase in durability factor with the presence of silica fume (Kashi and Weyers 1989).

The increase in silica fume from 0 to 10% causes a decrease in the durability factor from 94 to 85 at 210 cycles for mixtures with a water to cement ratio of 0.5 (Sabir 1997). The resistance to freezing and thawing was found to be reduced with the addition of silica fume in non-air entrained mixtures possibly due to the variance in the amount of High Range Water Reducer, however, when properly air entrained the silica fume had little to no effect (Cohen et al. 1992). With proper air entrainment and adequate strength of only 3500 psi before exposing to freezing and thawing there should be no significant difference in the resistance to freeze-thaw of concrete with or without fly ash. (ACI Committee 232 1996)

In tests performed by Ghosh and Nasser (1995) according to ASTM C-666, with a ternary blended cement having 10% silica fume, no air entrainment, and a water to binder ratio of 0.27, the addition of fly ash caused a reduction in the freeze-thaw resistance of the mixtures. The mixtures having 40% or more fly ash performed poorly with durability factors less than 60.

Cramer (2001) reported results in 2001 for 12 different fly ash mixtures with a water to binder ratio less than or equal to 0.45. The durability factor was 94 with or without 19% fly ash. This indicates that freeze-thaw durability is largely dependent on air entrainment.

The presence of slag in mixtures with up to 50% replacement of Portland cement gave durability factors greater than 90 provided the air content of these mixtures was greater than 3%. The slag mixtures seemed to be more susceptible to surface damage and weight loss than similar mixes with 19% Fly Ash. (Cramer 2001)

2.3.3 Effects of Water to Binder Ratio

The literature suggests that with a low water to binder ratio, a high strength concrete that is freeze-thaw resistant can be produced. The Durability factor is increased by about 30 with a decrease in the water to binder ratio from 0.40 to 0.35 for the control mixes and the mixtures containing 5% silica fume. This seems to have the greatest effect on the durability factor (Ozyildirim 1987).

2.3.4 Effects of Curing Time

Before specimens are subjected to the actual freeze-thaw test, the curing time and method have been varied so that the effects of curing on freeze-thaw resistance of the concrete can be examined. ASTM C-666 specifies that specimens be cured for only 14 days before exposure to freeze-thaw. There are arguments suggesting that this time is not long enough especially in some mixtures containing fly ash. The effect of curing on freeze-thaw resistance seems to be very small in most cases. There is only a slight increase in durability factor of the mixes that performed relatively well for a 12 hr heat cure at 65° C over a 23° C lime-water bath (Mokhtarzadeh 1995). An increase in moist cure time from 14 to 28 days doesn't cause a significant increase in the durability factor. However, it is important to recognize that these mixtures all had cementitious material contents of at least 822 lb/yd^3 (Kashi and Weyers 1989). Effects of moist curing in lime water were examined using different periods of time before exposing to the freeze-thaw test. In the air-entrained concrete there did not seem to be a major difference between curing times. For the non-air entrained mixes there was a greater difference between the relative dynamic modulus for specimens cured for different periods especially between 7

and 21 days. Longer curing times did not appear to have a large effect in freeze-thaw resistance (Cohen et al. 1992).

CHAPTER 3 EXPERIMENTAL PROGRAM

3.1 Mixes and Test Parameters

The twenty-four mixes used in the study were designed to study the effects of paste content, water to binder ratio, cement composition, and moist curing time. However, to limit the number of mixes in observance of completion time, paste content was eliminated as a variable and set at 0.25. Table 3.1 summarizes the test parameters that were used and the actual variations of each.

Table 3.1: Test variables used to develop mix designs.

Parameters	Variations
Water/binder ratio	0.25, 0.30, 0.35, 0.40
Silica Fume %	0%, 5%, 10%
Fly Ash %	0%, 25%, 50%

To test the effects of water to binder ratio, a set of five common mixes was tested for each of the water to binder ratio values listed in Table 3.1. The group included a control mix having no supplementary cementitious materials, a 25% fly ash mix, a 5% silica fume mix, a 10% silica fume mix, and a ternary blended mix having 5% silica fume and 25% fly ash. Four additional mixes were added to the 0.3-w/b series to test effects of cement composition in ternary blended mixes in further detail. Table 3.2 summarizes the values for water to binder ratio and cement composition parameters for each mix tested.

In addition to testing cement composition and water to binder ratio, moist curing time was tested to observe the pore structure development with time. Strength and

chloride penetration tests were conducted for each mix after 7, 28, and 56 days of moist curing.

Table 3.2: Summary of mixes and parameters for each

Mix #	Water/ binder	Silica Fume %	Fly Ash %
1	0.25	0	0
2	0.25	0	25
3	0.25	5	0
4	0.25	5	25
5	0.25	10	0
6	0.3	0	0
7	0.3	0	25
8	0.3	0	50
9	0.3	5	0
10	0.3	5	25
11	0.3	5	50
12	0.3	10	0
13	0.3	10	25
14	0.3	10	50
15	0.35	0	0
16	0.35	0	25
17	0.35	5	0
18	0.35	5	25
19	0.35	10	0
20	0.4	0	0
21	0.4	0	25
22	0.4	5	0
23	0.4	5	25
24	0.4	10	0

3.2 Mix Design

The design of each mix began with a constant paste content (water + cement + supplementary cementitious materials) of 0.25 by weight of the total mix. The weight of

cement and water was adjusted based on the specified water to binder ratio. The remainder of the mixture consisted of an equal weight of fine and course aggregate. Superplasticizer and air entraining agent were added based on experience and trial mixing prior to beginning the test program. Table 3.3 details the actual weights of the mixture components used on a per cubic yard basis.

Table 3.3: Design batch quantities per cubic yard

Mix	W_{Water} lbs/yd^3	W_{Sand} lbs/yd^3	W_{Gravel} lbs/yd^3	W_{Cement} lbs/yd^3	W_{Ash} lbs/yd^3	W_{Fume} lbs/yd^3	V_{SP}[(1)] oz/cwt	V_{AE}[(2)] oz/cwt
1	200.2	1501.5	1501.5	800.8	0.0	0.0	20	0.8
2	198.8	1491.2	1491.2	596.5	198.8	0.0	10	0.7
3	199.3	1495.1	1495.1	757.5	0.0	39.9	10	0.7
4	198.0	1484.8	1484.8	554.3	198.0	39.6	13	0.7
5	198.5	1488.6	1488.6	714.5	0.0	79.4	16	0.7
6	228.2	1483.0	1483.0	760.5	0.0	0.0	7.5	0.7
7	226.7	1473.3	1473.3	566.7	188.9	0.0	9.0	0.7
8	225.2	1463.7	1463.7	375.3	375.3	0.0	3.0	0.7
9	227.2	1477.0	1477.0	719.5	0.0	37.9	9.0	0.7
10	225.7	1467.3	1467.3	526.7	188.1	37.6	7.0	0.7
11	224.3	1457.8	1457.8	336.4	373.8	37.4	7.0	0.7
12	226.3	1470.9	1470.9	678.9	0.0	75.4	12.0	0.7
13	224.8	1461.4	1461.4	487.1	187.4	74.9	9.0	0.7
14	223.4	1451.9	1451.9	297.8	372.3	74.5	5.0	0.7
15	253.4	1466.3	1466.3	724.1	0.0	0.0	3.5	0.7
16	251.9	1457.2	1457.2	539.7	179.9	0.0	1.5	0.7
17	252.4	1460.6	1460.6	685.2	0.0	36.1	6.0	0.7
18	250.9	1451.5	1451.5	501.8	179.2	35.8	3.5	0.7
19	251.5	1454.9	1454.9	646.6	0.0	71.8	10	0.7
20	276.4	1451.1	1451.1	691.0	0.0	0.0	2.0	0.7
21	274.8	1442.5	1442.5	515.2	171.7	0.0	0.0	0.6
22	275.4	1445.7	1445.7	654.0	0.0	34.4	3.0	0.7
23	273.7	1437.1	1437.1	479.0	171.1	34.2	1.0	0.6
24	274.3	1440.3	1440.3	617.3	0.0	68.6	6.5	0.7

(1) Volume of superlasticizer added in ounces per hundred weight of cementitious material
(2) Volume of air entraining agent added in ounces per hundred weight of cementitious material

3.3 Constituent Material Properties

The coarse aggregate used was ¾" crushed limestone acquired from the local quarry. The fine aggregate used was locally available river sand. The Portland cement used was Ash Grove Type I/II, which meets the requirements for both ASTM C-150

Type I and Type II. Class C fly ash was obtained from Mineral Resource Technologies in Labadie, MO. Table 3.4 provides the chemical composition for the fly ash used. Force 10,000D available from W.R. Grace was the silica fume utilized. AdvaCast 530 also from W.R. Grace was the superplasticizer used. It is a polycarboxylate based superplasticizer design to comply with ASTM C-494 as a Type F admixture and ASTM C-1017. The air-entraining agent was Daravair 1000, also a W.R. Grace product. It is formulated from resin acids and rosin acids in an aqueous solution.

Table 3.4: Chemical composition for fly ash used

Compounds	Fly Ash
SiO_2	33.08%
Al_2O_3	22.76%
Fe_2O_3	6.29%
CaO	24.99%
MgO	5.06%
SO_3	2.27%
Loss on Ignition	0.36%
Specific Gravity	2.73

3.4 Specimen Preparation

The mixing was performed in a portable rotating drum mixer with a capacity of approximately 2 ft^3. All of the materials were weighed according to the mix design and volume required. Air entraining agent was added to the mix water. The aggregates, mix water, and air-entraining agent were added to the mixer first and allowed to mix for approximately one minute. Following adequate mixing of the water and aggregates, the cementitious materials were added slowly until the flow began to decrease. Superplasticizer was added as needed to maintain flow in the mixer. Trial mixes were cast to properly estimate the amount of superplasticizer required. The amount to add was

based on experience and the amount needed for mixes with similar compositions. After all of the materials were added, they were allowed to mix for approximately five minutes to ensure adequate flow and effectiveness of the superplasticizer. Testing of fresh concrete properties including slump, air content, and unit weight began immediately following mixing.

Specimens to be used for testing strength and chloride penetration and freeze-thaw resistance were cast after testing fresh concrete properties. Table 3.5 outlines the specimens that were cast and their uses. Twelve 4 in. x 8 in. cylinders were cast according to ASTM C-31. These specimens were then capped with plastic lids and properly labeled. The 3 in. x 4 in. x 16 in. prisms were consolidated in two equal layers on the vibrating table and finished with a strike-off plate. They were then covered with plastic to prevent rapid evaporation and exposure to water droplets in the curing room. The specimens were placed in the moist curing room immediately following casting.

Table 3.5: Summary of specimens cast and uses

Test	Specimen Type	Specimen Use	Specimen Total
Strength	4 in. x 8 in. Cylinder	2 tests at each age	6
Chloride penetration	4 in. x 8 in. Cylinder	2 tests at each age	6
Freeze-thaw	3 in. x 4 in. x 16 in. Prism	2 begin at 28 days	2

3.5 Curing

All specimens were cured in a moist curing room having a relative humidity of 100% and temperature of approximately 70° F. The 4 in. x 8 in. cylinders to be used for strength and chloride penetration were allowed to cure in the plastic cylinder molds with caps until the day of testing. These specimens were left in the molds to prevent them from rapidly drying out in the event of failure of the atomizers, which supply the curing

room with constant 100% relative humidity. The prisms to be used for freeze-thaw testing were removed from the steel molds on the day following casting. These specimens were marked and immediately returned to the moist curing room until testing began after 28 days.

CHAPTER 4 EQUIPMENT AND PROCEDURE

4.1 Chloride Penetration Test

All chloride penetration tests in this study were conducted according to ASTM C-1202 or AASHTO T-277, the Standard Test Method for Electrical Indication of Concrete's Ability to Resist Chloride Ion Penetration. All of the equipment and setup to complete this test was designed and constructed according to the standard.

4.1.1 Test Setup

A regulated 60V DC power supply and automated current measuring system with data acquisition was built with the capacity to test twelve specimens simultaneously. This allowed for testing six specimens from each of two mixes on a single day. The entire test setup is shown in Figure 4-1. The power supply consisted of a 0-120V variable AC voltage transformer, an isolation transformer, and a rectifier with 10,000 μF capacitance for converting the AC voltage to DC. The unregulated DC voltage was then supplied to each individual channel, where the voltage was regulated to the constant 60V ±0.1V. The voltage regulation on each channel was accomplished using Texas Instruments TL783C voltage regulators, which are adjustable up to 125V. Each channel also had its own circuit for measuring and recording the values for the electrical current measured across the specimens.

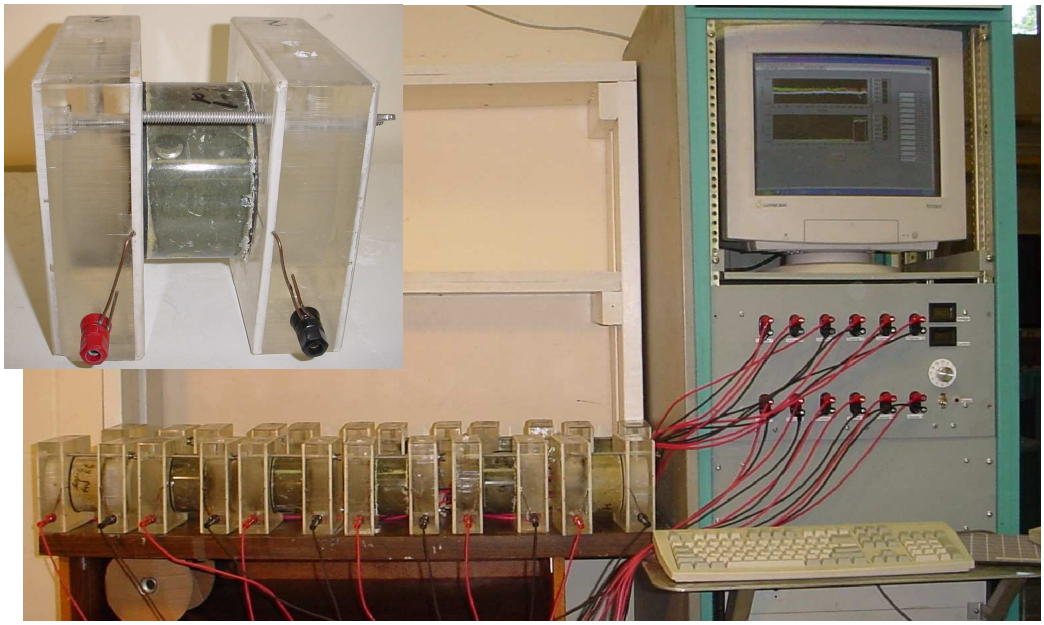

Figure 4-1: Rapid chloride penetration test setup

A computer data acquisition system (DAQ) was used to record the data for the electrical current measured across the chloride permeability specimens. The data acquisition used a National Instruments DAQ card and LabVIEW software to obtain the data. The DAQ card input requires a 0-10V analog DC signal. Current sensors manufactured by F.W. Bell were employed to convert the current value measured across the specimen to a DC voltage. This voltage was calibrated to the exact current measured across the specimen with an ammeter. The gain and offset of the voltage was adjusted using an amplifier circuit on each channel. The voltage output of the amplifier circuit was connected to the DAQ card. National Instruments LabVIEW software was written to acquire data over the six-hour test duration. The user interface portion of the software is shown in Figure 4-2.

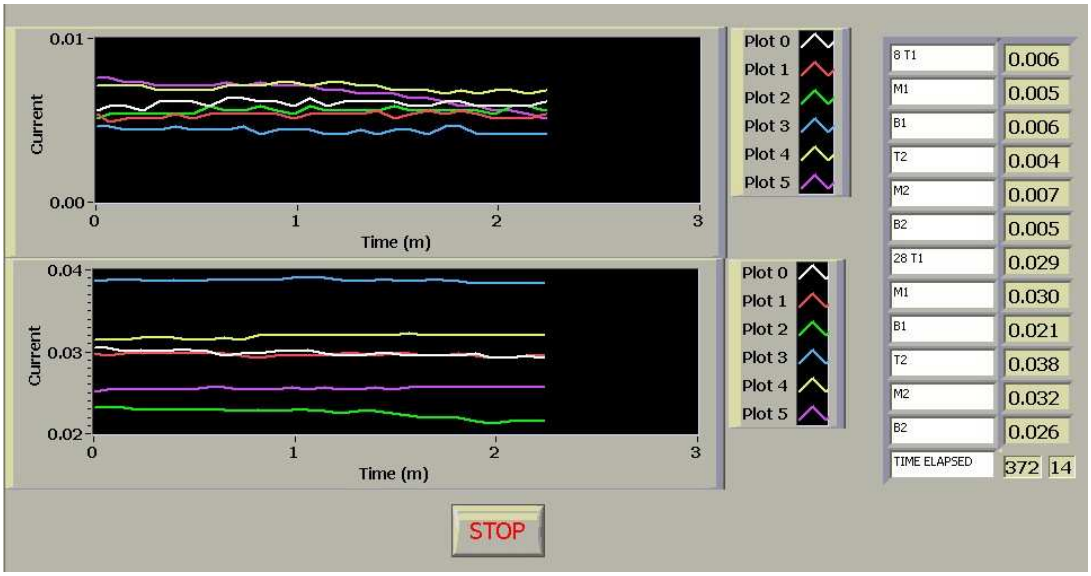

Figure 4-2: Front panel display of LabVIEW data acquisition program for RCPT

The total electrical charge passed through the specimen was found by calculating the area under the time-current plot using the trapezoidal rule. Current across the specimens was measured at 5-second intervals over the entire 6-hour test period and displayed on the plot shown in Figure 4-2. The measured current of each channel and the corresponding time was written to a spreadsheet file every 10 minutes. Table 4.1 outlines the qualitative terms set by ASTM for values of total charge passed.

Table 4.1: ASTM designation for chloride ion penetrability based on charge passed

Charge Passed (Coulombs)	Chloride Ion Penetrability
>4,000	High
2,000-4,000	Moderate
1,000-2,000	Low
100-1,000	Very Low
<100	Negligible

4.1.2 Specimen Conditioning

Two days prior to the actual chloride penetration testing, two cylinders from each mix were removed from the moist curing room and de-molded. The sides of the specimens were then sealed using a two-part epoxy sealant called PolyCarb. The epoxy was allowed to cure overnight. On the day prior to the tests, the specimen conditioning process was completed. Three specimens were cut from each cylinder using a portable masonry saw. Approximately 0.5 in. was sliced from the top of the specimen. Then three equal 2 in. specimens were sliced from each cylinder, allowing for six specimens from each mix to be tested on each test day. Figure 4-3 illustrates how the specimens were cut for the RCPT.

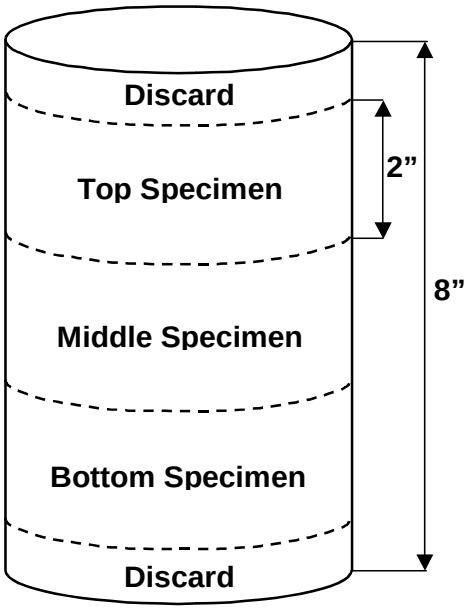

Figure 4-3: Diagram of specimen slicing to be used for the rapid chloride penetration test

Before the vacuum preparation process began, a sufficient volume of water to cover the specimens in the vacuum desiccator was de-aired. To de-air the water, it was boiled vigorously, then removed from the heat, sealed from the outside environment with

the boiling pot lid, and allowed to cool to room temperature. The specimens were then placed in the vacuum dessicator shown in Figure 4-4 for three hours. At the end of three hours, the de-aired water was drawn into the vacuum chamber until the specimens were covered. After one hour of vacuuming under water, air was allowed to re-enter the chamber. Specimens then soaked under the same water for 18 ± 2 hours prior to beginning the actual test.

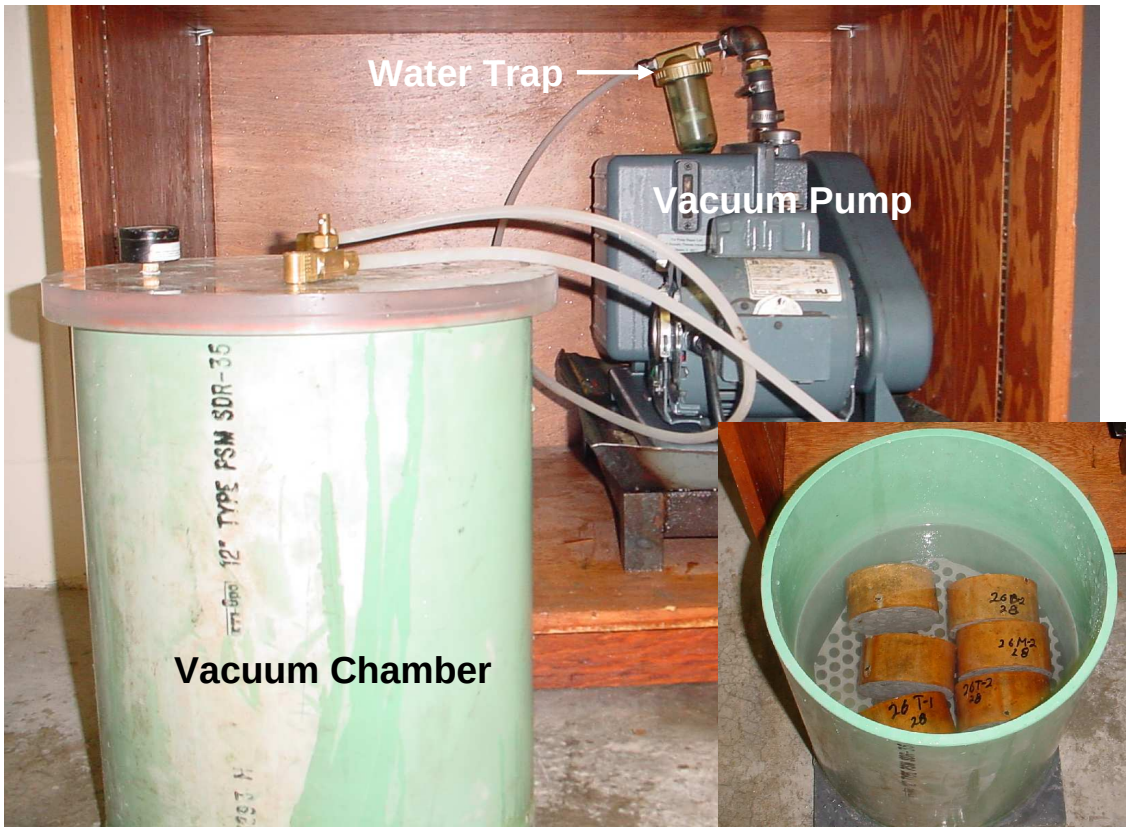

Figure 4-4: Photograph of the rapid chloride penetration test specimen conditioning equipment, Inset: Specimens stacked in the Vacuum Chamber

4.1.3 Procedure

Following the entire specimen conditioning process, the specimens were taken from the vacuum chamber, and the excess water was removed from the surface. The

specimens were then placed into the cells with rubber gaskets between the specimen and the brass terminal in each side of the cell to seal them from leaking. After the cells were bolted together, as pictured in Figure 4-1, the side connected to the positive terminal of the power supply was filled with 0.3N NaOH, and the side connected to the negative terminal was filled with 3.0% NaCl Solution. Before the specimen's electrical leads were plugged into the terminals on each channel, the voltage of each channel was checked to ensure that it was equal to 60.0 V, and the offset for the data acquisition of current was verified to be zero. The specimens were finally connected to the 60 V, and the data acquisition program was started. At the end of the 6-hour test, the power was switched off and the DAQ was stopped. The calculation of total charge passed was completed using Microsoft Excel.

4.2 Freeze Thaw Test

The freeze-thaw tests were conducted according to Procedure A of ASTM C-666, the Standard Test Method for resistance of concrete to rapid freezing and thawing.

4.2.1 Test Setup

The freeze-thaw tests were conducted in a cabinet with a capacity of 18 specimens, pictured in Figure 4-5. Specimens were held inside stainless steel containers with at least 0.125 in. of water completely surrounding them. The cabinet uses a single cooling unit and resistance-type strip heaters between the specimens to complete approximately nine freeze-thaw cycles per day. A single specimen that was not being tested was used for temperature control with two thermocouples inside to measure temperature at the center of the specimen. One thermocouple was connected to the

temperature control circuit, while the other was connected to a chart recorder to observe the actual temperature and to keep record of the number of cycles.

Figure 4-5: Freeze-thaw cabinet shown during thawing portion of a cycle

4.2.2 Procedure

The specimens used for this test were 3 in. x 4 in. x 16 in. prisms. Testing began on the freeze-thaw specimens after a period of 28 days of moist curing. Immediately following removal of the specimens from the curing room, they were brought to a temperature of approximately 40 °C by placing them in the cabinet for one cycle. Next, the specimens were removed from the cabinet, and the fundamental transverse frequency and weight were measured prior to starting the freeze-thaw cycles. This allowed a baseline dynamic modulus of elasticity to be calculated. Specimens were also removed from the freeze-thaw cabinet at intervals of approximately every 30 cycles to measure the fundamental transverse frequency and weight of each specimen. The specimens were

returned to the cabinet in reverse order and turned over to provide even exposure to all specimens.

The fundamental transverse frequency was measured according to ASTM C-215 using the equipment shown in Figure 4-6. The frequency was adjusted until the electro-mechanical driving unit pictured on the left end of the specimen and the pickup needle on the right end were in phase. The oscilloscope on the control console indicated when the ends of the specimen were in phase, or the fundamental transverse frequency had been reached. The weight of each specimen was also recorded in order to calculate the dynamic modulus of elasticity. The relative dynamic modulus of elasticity is the ratio of the dynamic modulus at a given number of cycles to the original dynamic modulus. The relative modulus is then used to calculate the durability factor. The durability factor is defined as the relative dynamic modulus of elasticity times the ratio of the number of cycles at which the test was discontinued to the specified number of cycles for terminating freeze-thaw exposure. This value is then multiplied by 100 to give a value in percent.

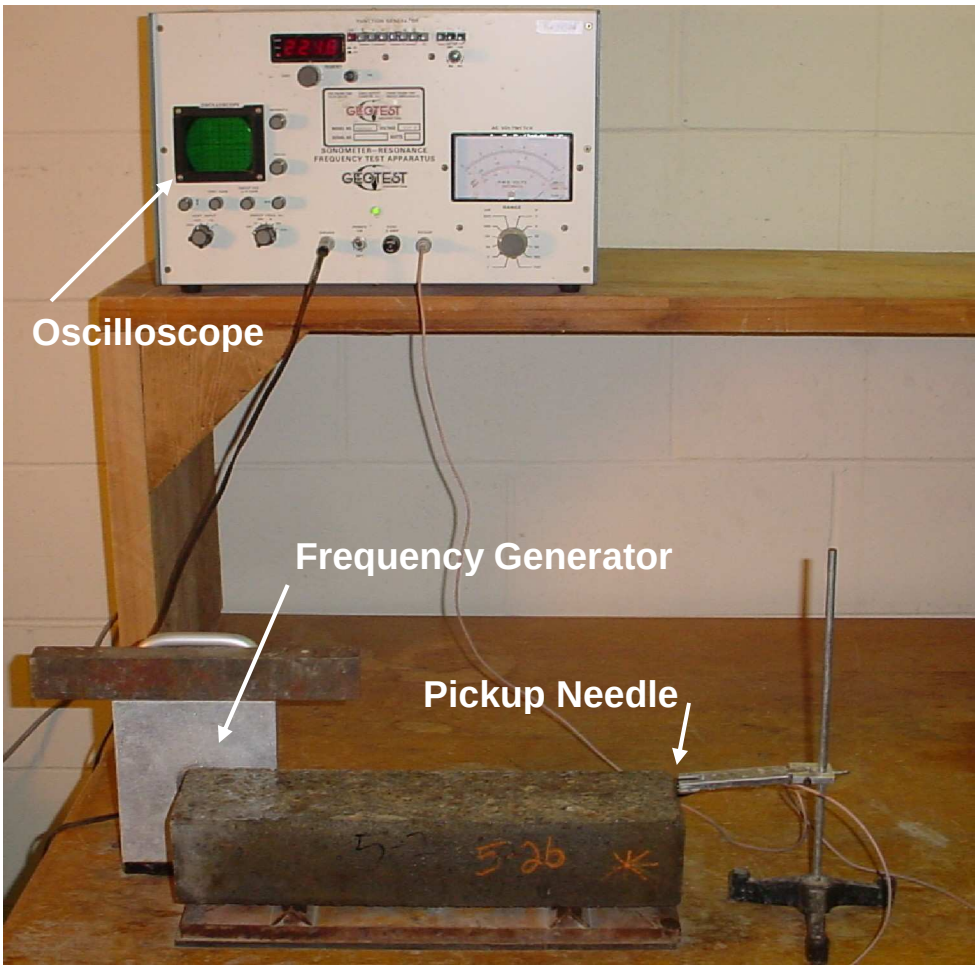

Figure 4-6: Frequency generator and setup for measuring fundamental transverse frequency

4.3 Compressive Strength Test

The compressive strength of each mix was tested at 7, 28, and 56 days of moist curing. The tests were performed according to ASTM C-39, the Standard Test Method for Compressive Strength of Cylindrical Concrete Specimens. The 4 in. x 8 in. cylindrical specimens were first capped using sulfur mortar capping compound to ensure parallel and smooth ends. This procedure was performed in accordance with ASTM C-617, Standard Practice for Capping Cylindrical Concrete Specimens. The Forney concrete compression-testing machine pictured in Figure 4-7 was used for the actual

compression tests. The specimens were loaded at a rate of 45-50 psi/s in accordance with ASTM C-39.

Figure 4-7: Photograph of concrete cylinder compression testing machine

CHAPTER 5 TEST RESULTS AND DISCUSSION

5.1 Fresh Concrete Properties

Immediately following concrete mixing, fresh concrete properties including slump, unit weight, and air content were measured and recorded. The results of these tests are listed in Table 5.1. Air content was measured using the pressure method according to ASTM C-231 (2003b). Unit weight was measured according to ASTM C-138 (2001) using the 0.25 ft^3 pot from the air content measuring apparatus. Slump was measured using the standard method according to ASTM C-143 (2003a) for the majority of mixtures. However, a few mixtures required measurement of slump flow when the slump was too high to be measured using the standard test. The slump flow test, typically used for self-consolidating concrete (SCC), is a measure of the viscosity of the concrete mixture. The slump flow test measures the time taken for the concrete to reach a spread diameter of 30 inches from the instant the standard slump cone is lifted. This test allowed a measure of the workability for the mixtures that would be considered a self consolidating concrete.

Table 5.1: Properties measured on fresh concrete

Mixture	Slump (in.)	Unit Weight (lbs/ft^3)	Air Content (%)
1	25s[1]	150.0	4.0
2	23s[1]	147.6	4.7
3	8.0	149.2	4.0
4	8.0	146.0	5.3
5	2.5	148.8	4.2
6	5.5	145.2	5.5
7	12s[1]	142.0	6.0
8	5.5	140.8	6.8
9	2.3	145.6	5.1
10	3.0	143.6	6.1
11	8.0	138.8	7.5
12	4.0	146.0	4.5
13	2.0	145.2	4.5
14	7.0	137.6	7.0
15	2.0	144.8	4.5
16	4.5	143.6	5.6
17	8.0	144.8	6.0
18	8.0	137.6	7.5
19	8.0	142.0	5.7
20	3.0	143.2	5.2
21	5.5	144.0	4.5
22	7.5	136.4	7.5
23	3.3	144.0	4.2
24	6.5	132.4	10.0

[1]Slump Flow Measured

The fresh concrete properties are not the focus of this report, but can be useful in analyzing some of the freeze-thaw and compressive strength results. Though the trend may not readily appear in Table 5.1, it was noticed during mixing and casting that the workability generally increased with fly ash use and decreased with the use of silica fume. Superplasticizer was used to adjust the slump to a workable level depending on the

mixture. The slump results are reported in the table above; however, these values should not be considered a result of the concrete mixtures, as this value could easily change with the amount of superplasticizer used.

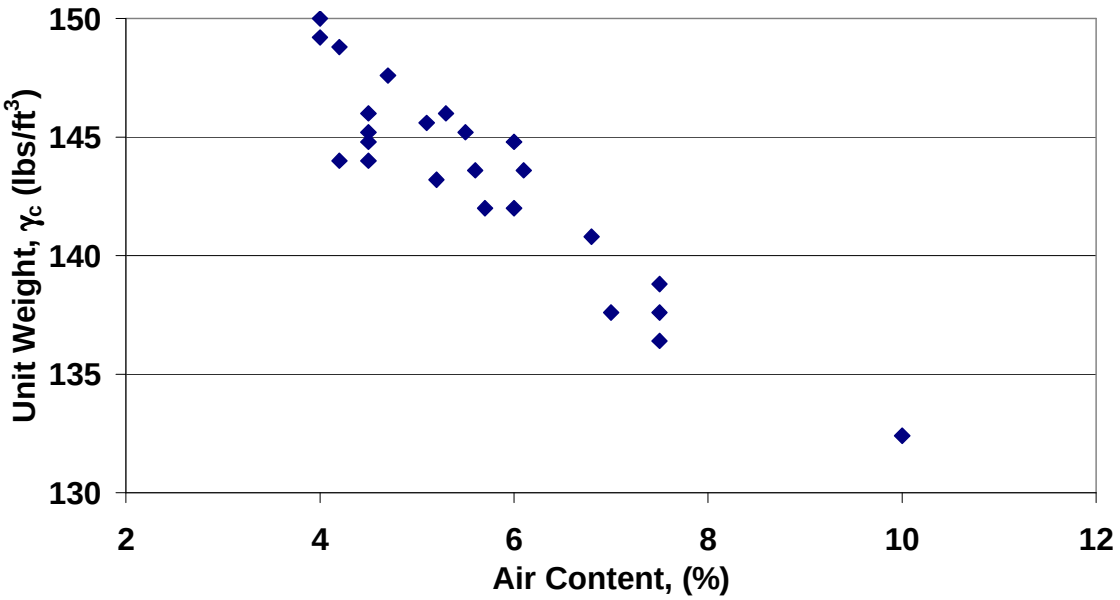

Figure 5-1: Effect of air content on unit weight of fresh concrete

A target air content of 4 to 7% was used to provide adequate protection against freeze-thaw damage, based on the results of the literature review completed prior to testing. With a few exceptions, as seen in Figure 5-1, the target air content was achieved. As expected, the unit weight of the fresh concrete was indirectly proportional to the air content, also seen in Figure 5-1. Higher air contents and resulting in lower unit weights can be useful in understanding the compressive strength results. Compressive strength values that are lower than expected compared to similar mixes may possibly be explained by higher air content.

5.2 Compressive Strength

The compressive strength results are not the focus of this study; however, these results can be useful in the investigation of pore structure development and its

relationship to durability in the different mixture types. The effects of water to binder ratio, cement composition, and moist cure time were studied on the compressive strength of all mixtures. The results of the compressive strength tests are reported in Sections 5.2.1 through 5.2.3.

5.2.1 Effect of Water to Binder Ratio

The plots below illustrate the effects of water to binder ratio on all mixtures tested. The results are plotted at the three curing times tested. These plots compare the results of all the cement blends tested with the exception of 50% fly ash mixtures and the 10% silica fume ternary blends, which were added to the 0.30 w/b ratio series.

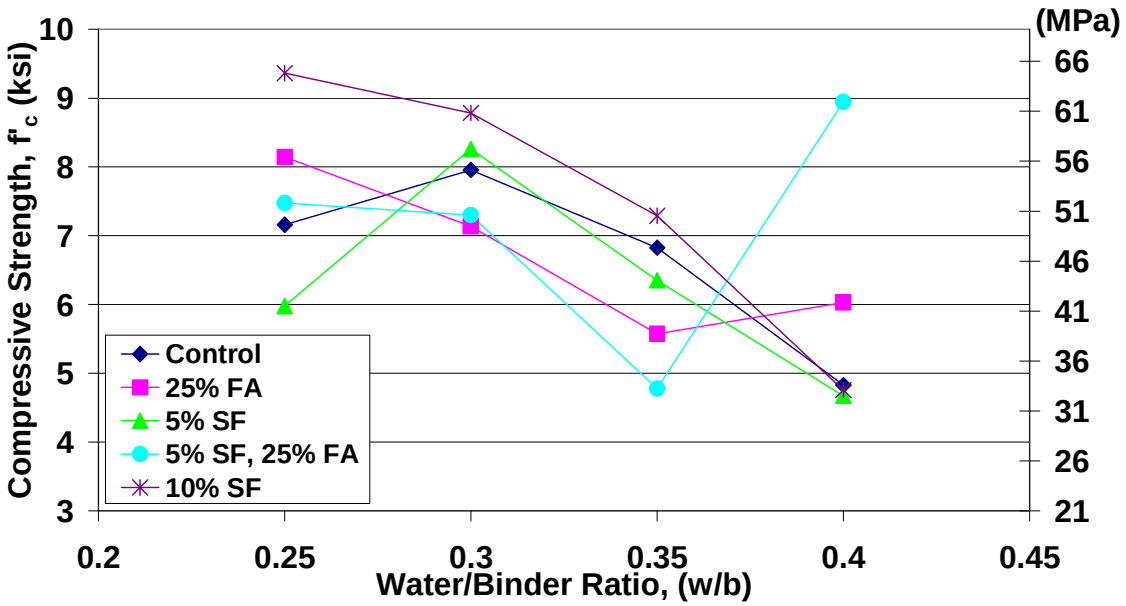

Figure 5-2: Influence of water to binder ratio on compressive strength at 7 days moist cure

The higher early strength of silica fume as compared to the fly ash and control can be seen in the 7 day results shown in Figure 5-2. There are two definite outliers that exist in this plot. The 5% silica fume, 0.25 w/b ratio mixture had an unexpected trend as the strength is approximately 2,000 psi less than the same mixture with 0.30 water to binder

ratio. This is possibly due to poor specimen preparation or testing error since the 28 and 56 day results for the same mixture give expected compressive strength results. Another exception to existing trends is the result of the ternary mixture with 0.40 water to binder ratio. There is an increase from approximately 4,800 to 9,000 psi for the water to binder ratio increase from 0.35 to 0.40. As evident by Figure 5-2, all other mixtures decreased in strength with the increased water to binder ratio.

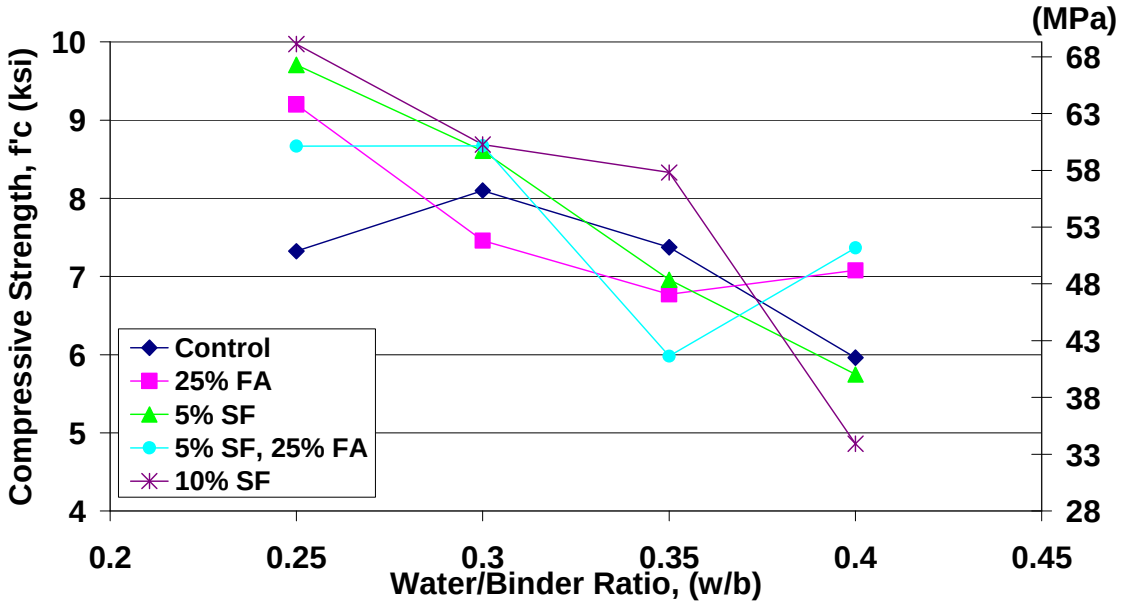

Figure 5-3: Influence of water to binder ratio on compressive strength at 28 days moist cure

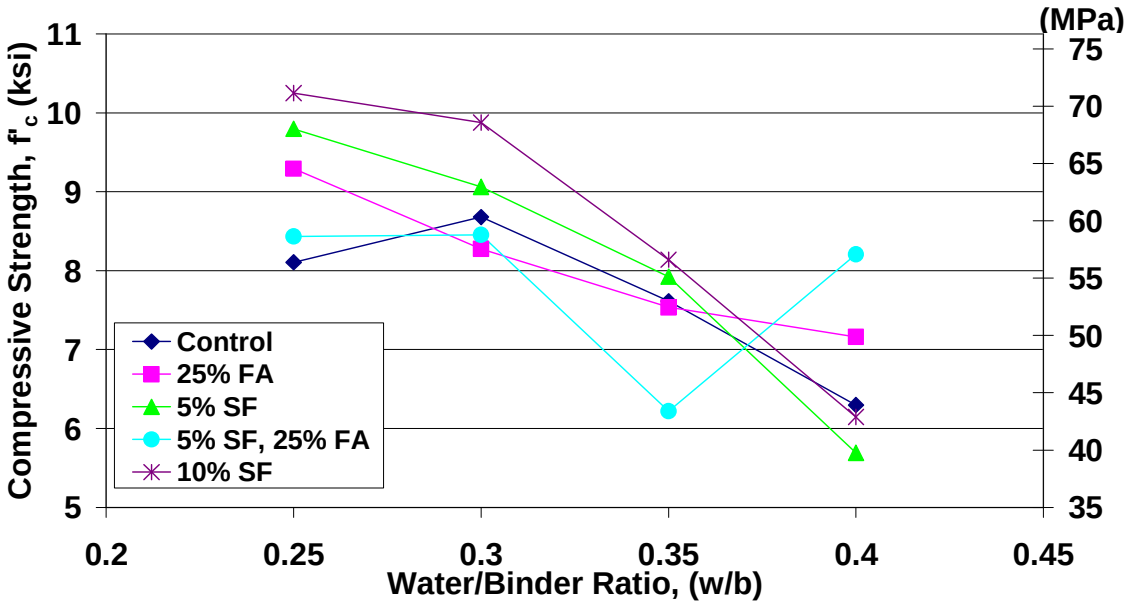

Figure 5-4: Influence of water to binder ratio on compressive strength at 56 days moist cure

A common trend exists among all ages of curing for the compressive strength versus water to binder ratio. The compressive strength is indirectly proportional to the water to binder ratio. This is the expected result as the water not used by the cement hydration process leaves voids in the concrete matrix, thereby decreasing the compressive strength. There is a common outlier that exists in the data at all ages that requires explanation. For the ternary mixture at all ages of moist curing, as the w/b ratio increased from 0.35 to 0.40, the compressive strength increased rather than decreased as with the other mixtures. This unexpected result can possibly be explained by the difference in air content. As shown in Table 5.1, Mix 27, the 0.40 w/b mixture had an air content of 4.2, while Mix 22, the 0.35 w/b mixture had an air content of 7.5.

A common trend exists in the compressive strength results shown in Figure 5-2 through Figure 5-4. The increased void content resulting from increasing water to binder ratio is evident as the compressive strength decreases with water to binder ratio increase.

The effects of fly ash and silica fume tend to lessen as water to binder ratio increases. Some of the outliers make it difficult to see existing trends in the data shown in Figure 5-2 through Figure 5-4.

5.2.2 Effect of Cement Composition

The following plots compare compressive strength results for the ternary blended cement mixtures with a 0.30 w/b ratio at 7, 28, and 56 days of moist curing.

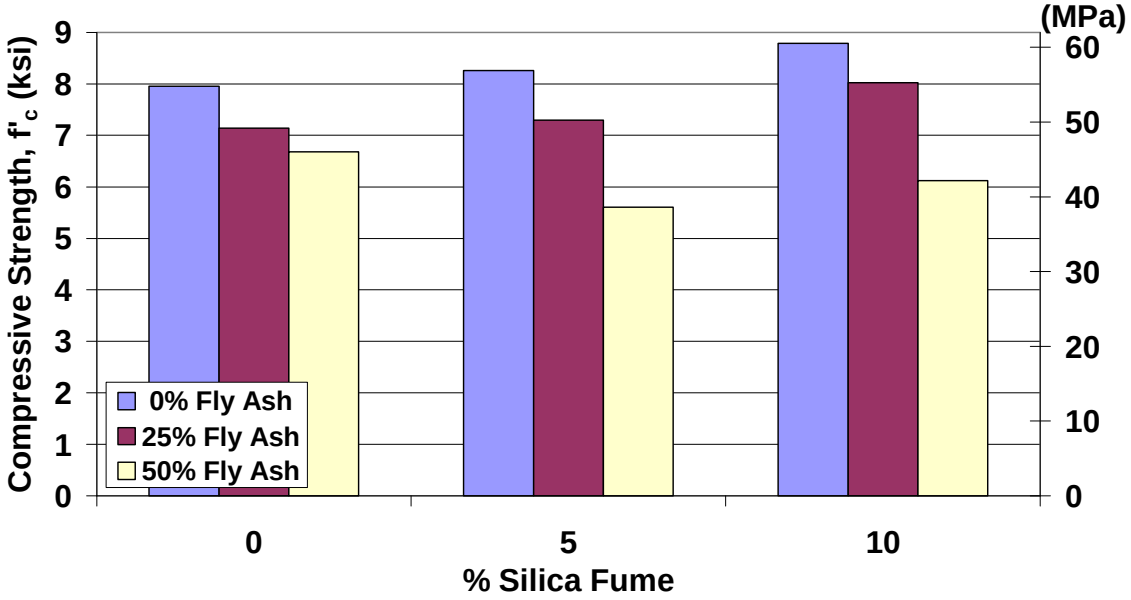

Figure 5-5: Influence of cement composition on compressive strength at 7 days moist cure for 0.3 w/b mixes

The slow reaction of fly ash is apparent in Figure 5-5. The 7 day compressive strength obviously decreases as the percentage of fly ash in the cement mixture increases. However, compressive strength does increase slightly as the amount of silica fume is increased except in the 50% fly ash mixtures. This increase in compressive strength for mixtures having either 0 or 25% fly ash is less than 1,000 psi as silica fume percentage is raised from 0 to 10%. Overall this strength increase is relatively small.

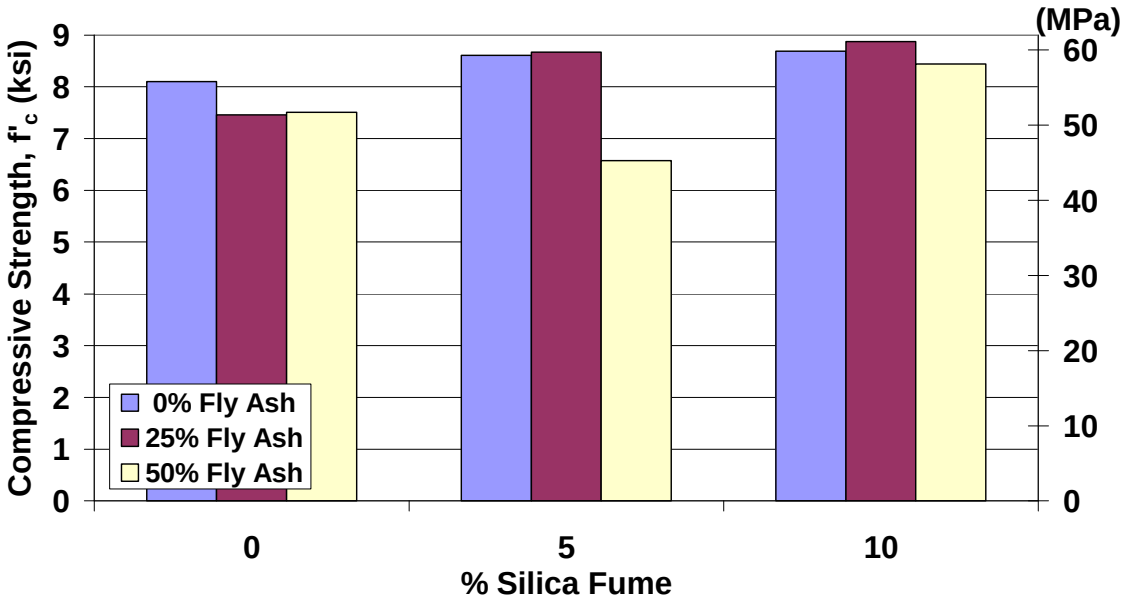

Figure 5-6: Influence of cement composition on compressive strength at 28 days moist cure for 0.3 w/b mixes

The increase from 5 to 10% silica fume results in a negligible increase in compressive strength except in the 50% fly ash mixtures.

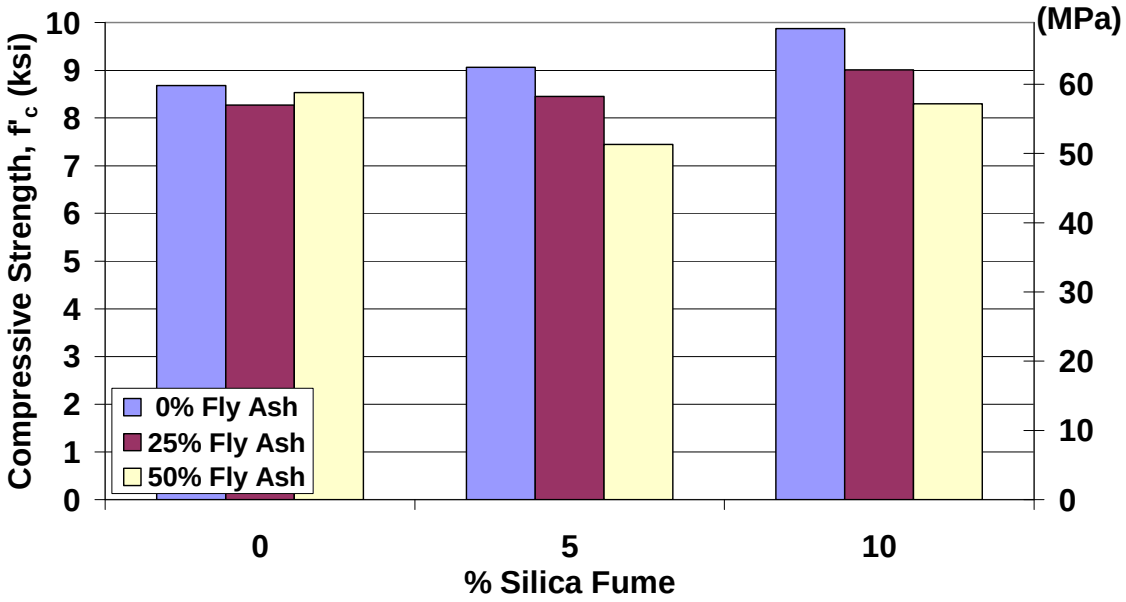

Figure 5-7: Influence of cement composition on compressive strength at 56 days moist cure for 0.3 w/b mixes

In the 50% fly ash mixtures, the compressive strength decreased as silica fume increased. A potential cause for this is the decrease in workability with addition of silica

fume. The higher silica fume specimens may not have been consolidated like the specimens having less silica fume, resulting in a compressive strength decrease.

5.2.3 Effect of Moist Curing Time

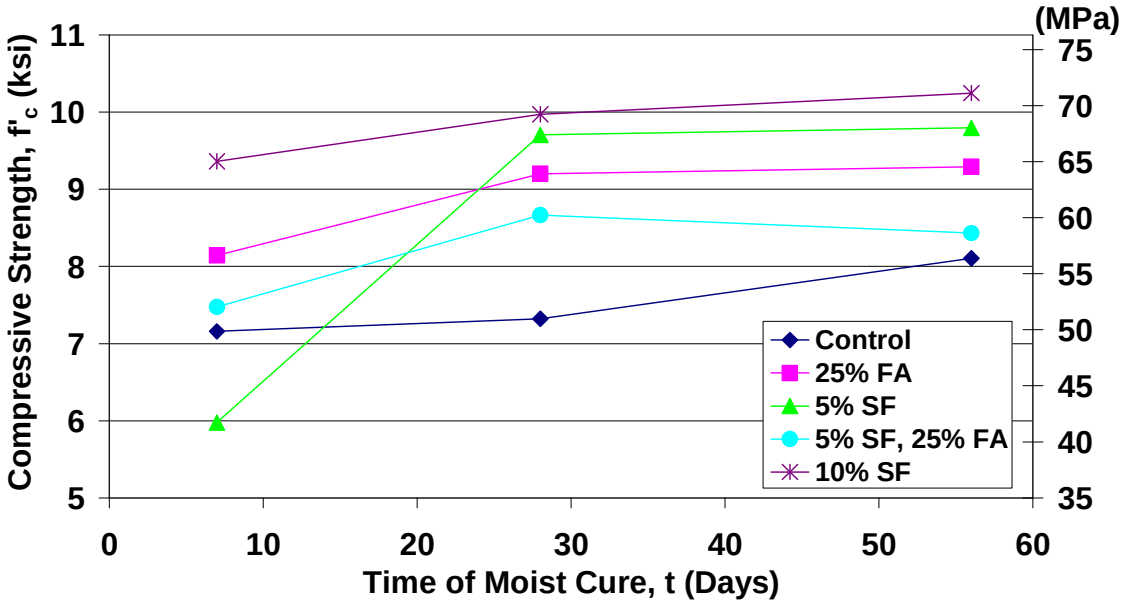

Figure 5-8: Influence of moist cure time on compressive strength of 0.25 water to binder ratio mixes

The addition of silica fume increased the compressive strength of the low water to binder ratio mixtures at all ages. The exception is the 5% Silica Fume mixture at 7 days of moist curing. This test was most likely erroneous due to the strengths being consistent with other mixtures at 28 and 56 days. Excluding the points at 7 days of moist curing, there is only a minor decrease in chloride permeability with the increase of silica fume from 5 to 10%. With the 0.25 water to binder ratio, both fly ash and silica fume increase the compressive strength compared to the control mixture. It can also be observed from Figure 5-8 that fly ash and silica fume alone perform better than the ternary mixture with regard to compressive strength.

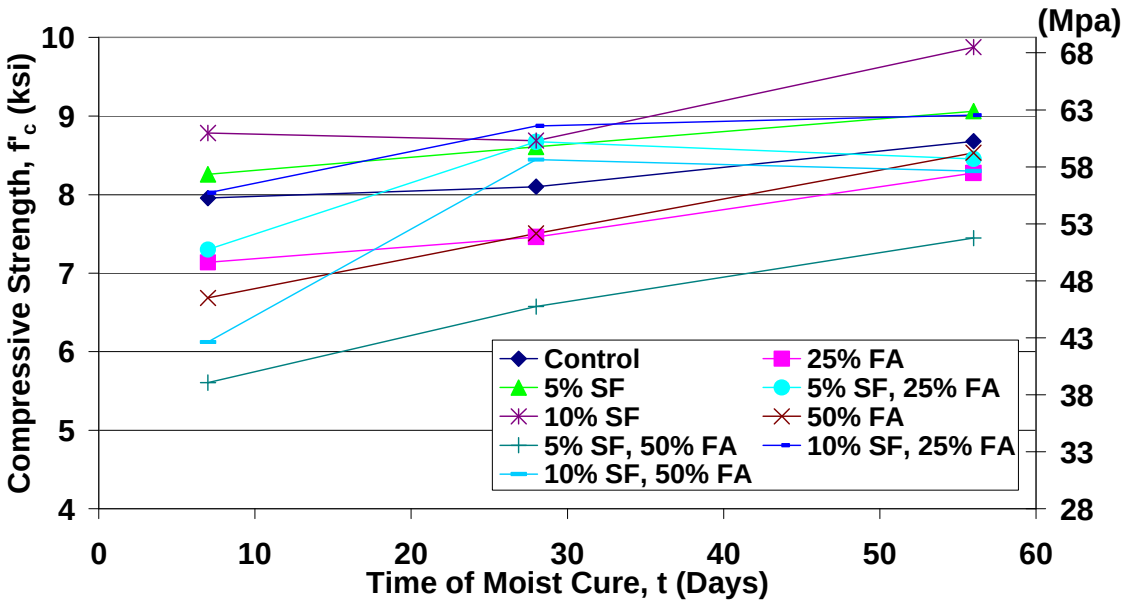

Figure 5-9: Influence of moist cure time on compressive strength of 0.3 water to binder ratio mixes

As the water to binder ratio increases from 0.25 to 0.30, the addition of silica fume and fly ash appear to have different effects. One important observation that can be noted from Figure 5-9 is that nearly all mixtures containing fly ash had 7-day strengths significantly less than the control mixture, but were nearly equal or higher after 56 days of curing. The one unexpected exception to this is the ternary blend having 5% silica fume and 50% fly ash. This mixture had compressive strengths consistently about 1,000 psi lower than the 50% fly ash alone. The results shown in Figure 5-9 indicate a negligible change in compressive strength from 25 to 50% fly ash among mixtures containing only fly ash and Portland cement. The mixtures shown in Figure 5-9 are also described in detail in Section 5.2.2.

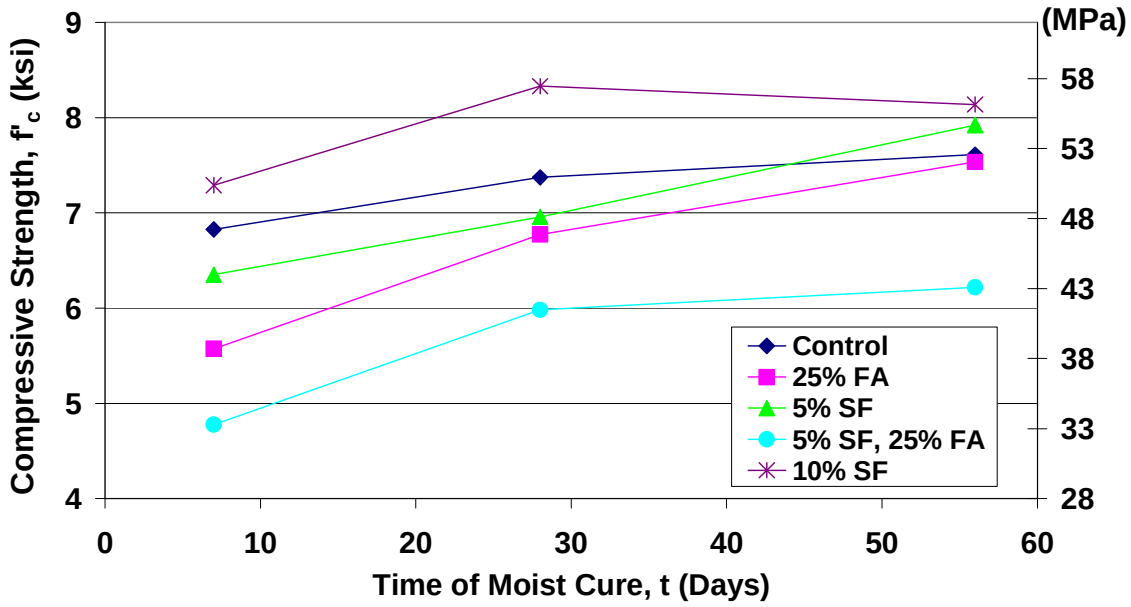

Figure 5-10: Influence of moist cure time on compressive strength of 0.35 water to binder ratio mixes

The compressive strength results for the 0.35 water to binder ratio mixtures are similar to the lower water to binder mixtures. The binary fly ash and silica fume mixtures have significantly better strength results than the ternary blended mixture as seen in the 0.25 water to binder series. Also indicated by Figure 5-10 is the 7 and 28 day compressive strength of the control mixture was greater than all other mixtures except for 10% silica fume.

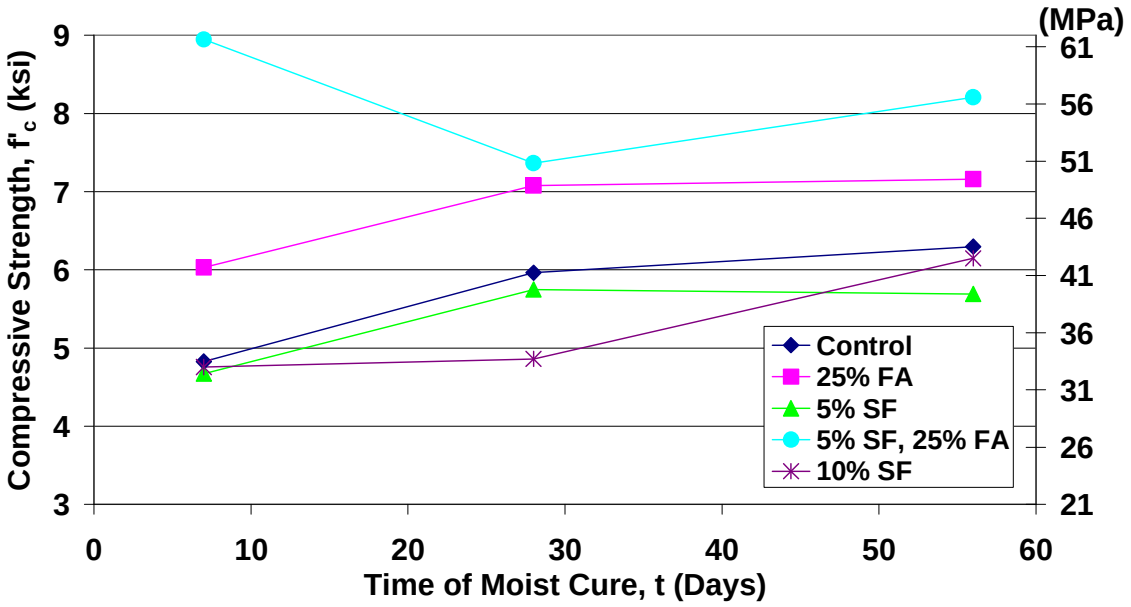

Figure 5-11: Influence of moist cure time on compressive strength of 0.40 water to binder ratio mixes

As the water to binder ratio increases to 0.40, the ternary blended mixture performs better than all other mixtures with respect to compressive strength. However, there is likely some error in the 28 day strength of this mixture. Figure 5-11 indicates the decrease in compressive strength from 7 to 28 days. It is also noted from the above graph that silica fume alone was not beneficial in increasing the compressive strength for the 0.40 water to binder mixtures. Figure 5-11 suggests that at the higher water to binder ratio fly ash becomes more effective at increasing compressive strength.

The common trend appears that compressive strength increases with moist curing time at all levels of water to binder ratio. The effects of curing time tend to be the lowest among the 0.25 water to binder ratio mixtures as seen in Figure 5-6. The plots tend to have less increase from 7 to 56 days.

The compressive strength plots provide some unexpected trends based on behavior of the different cement compositions. The results presented in these plots are somewhat inconclusive. Use of more than two test specimens at each test time may have

been useful in some cases to determine erroneous data points. Eliminating any data points caused by invalid compressive strength tests or improperly prepared specimens could potentially reduce the number of unexpected results like those shown in the above plots.

5.3 Chloride Permeability

As stated previously, all chloride penetration tests were conducted according to ASTM C-1202, commonly known as the Rapid Chloride Penetration Test (RCPT). There is a discussion of the time-current response during the RCPT and the effects of specimen heating during the six hour test. The effects of water to binder ratio, cement composition, and curing time are reported and discussed in detail in Sections 5.3.2 through 5.3.4.

5.3.1 Current vs. Time Response

The current versus time response varied greatly for the different types of mixtures tested. A study of the current vs. time plots assists in understanding RCPT results and how they are affected by different mixtures. The following plots are average current vs. time responses of six specimens from each mixture. The two plots shown are from the mixture with the least permeability and a mixture that was among those with the highest permeability.

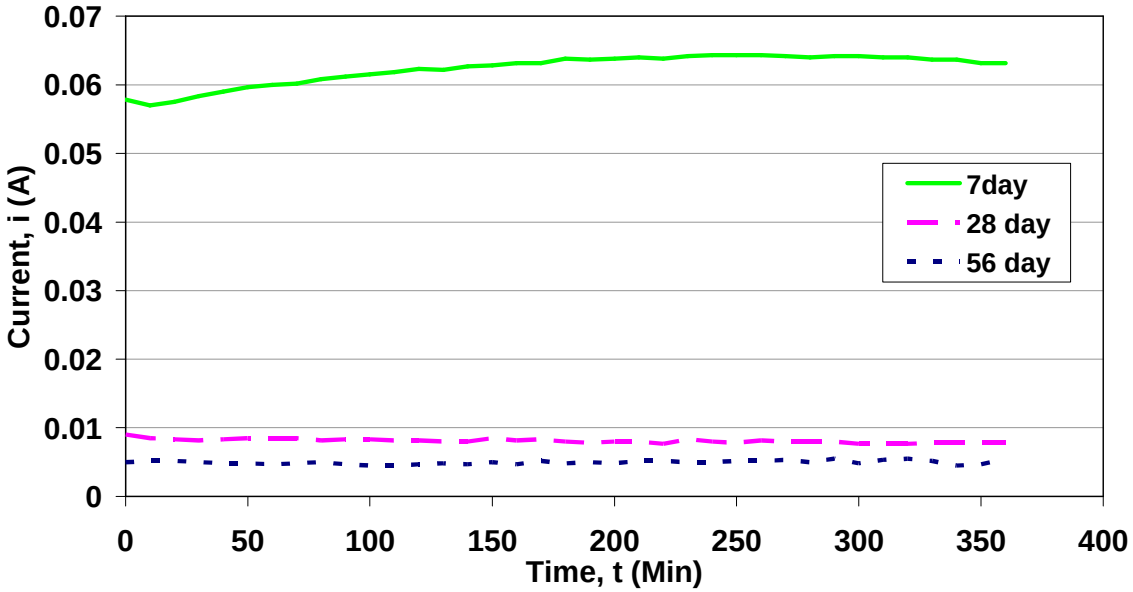

Figure 5-12: Time-Current response for Mix 5: 0.25 water to binder ratio, 10% silica fume

Mix 5 (0.25 w/b ratio, 10% silica fume) produced the lowest values for charge passed during the six-hour test at all ages. As shown in Figure 5-12, the current through the specimens decreased by a factor of 10 after 56 days of moist curing, compared to seven days of moist curing. Particularly interesting in the time vs. current plots is the shape of the curve. This is especially noticeable in the highly penetrable mixes. The total charge passed for Mix 11 was among the highest at all ages of moist curing. A large difference can be seen between Mixes 5 and 11 in the variation of current during the test. For Mix 5, the current varied about 10% throughout the 6-hour test. However, for Mix 11 the current ranged over 30% of the peak value, as seen in Figure 5-13.

The increase in current throughout the 6 hour test as shown in Figure 5-13 is common to specimens with high permeability. The higher current and resulting higher coulomb values are likely due to heating that occurs in the chloride solution and concrete specimens. The current generated by the applied voltage, generates heat as it flows through the conductor. Conductivity of electricity is affected by temperature. The heat

generated is proportional to the amount of charge passed through the specimen and the applied voltage by the formula, $J = EIt$, where J is the heat in joules, E is potential in volts, I is the current in amperes, and t is time in seconds. Increase in temperature increases the flow chloride ions which thereby increases the current passing through the specimen. This effect commonly known effect was studied and reported in detail by Julio-Betancourt (2004).

A look at the current values in Figure 5-12 and Figure 5-13 indicate that the values for the 10% Silica fume mixture are nearly an order of magnitude lower than those of the mixture containing 50% fly ash at all three ages. This is useful in describing the pore structure development of the different mixture types. Resistance of chlorides into concrete can be increased with the use of binary and ternary cement mixtures that include fly ash and silica fume (Bleszynski et al. 2002). Permeability is reduced by a finer pore structure created with the use of silica fume and fly ash. These supplementary cementitious materials react with calcium hydroxide (CaOH) formed during Portland cement hydration. Permeability is decreased as products from this secondary reaction are formed within the hardened structure reducing the size of the pores (Hooton 1986). Gopalaratnam et al. (2003). However, the reaction of fly ash is much slower than that of silica fume. This results in the much higher permeability of the 50% fly ash mixtures seen when comparing Figure 5-12 and Figure 5-13.

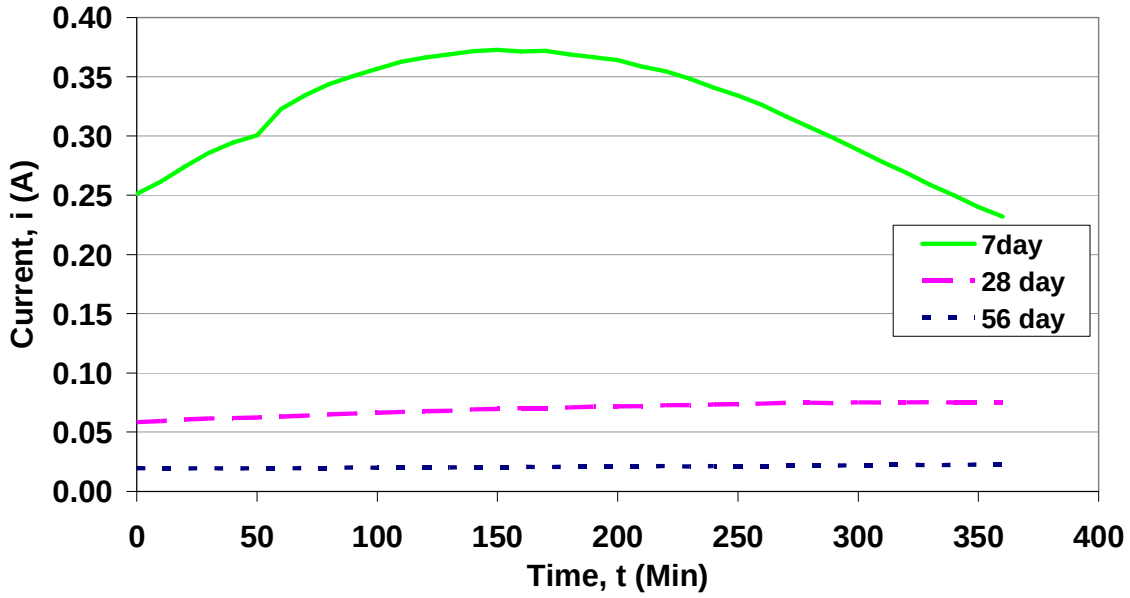

Figure 5-13: Time-Current response for Mix 11: 0.30 water to binder ratio, 5% silica fume, 50% Fly Ash

To achieve a more complete understanding of the chloride penetration during the test, a simple experiment was conducted on the RCPT specimens during a typical test. Two specimens were removed from the test after each hour during the six hour test. The profile of the chloride penetration was then observed. The specimens were split into two halves and sprayed with 0.1M silver nitrate solution. This process is similar to that used in the Rapid migration test to determine chloride penetration (AASHTO TP 64-03 2003). The white/gray silver chloride precipitate forms on the split surface indicating the depth of penetration as seen in Figure 5-14 and in Sections 5.3.3 and 5.3.4 as the mixtures are compared to each other.

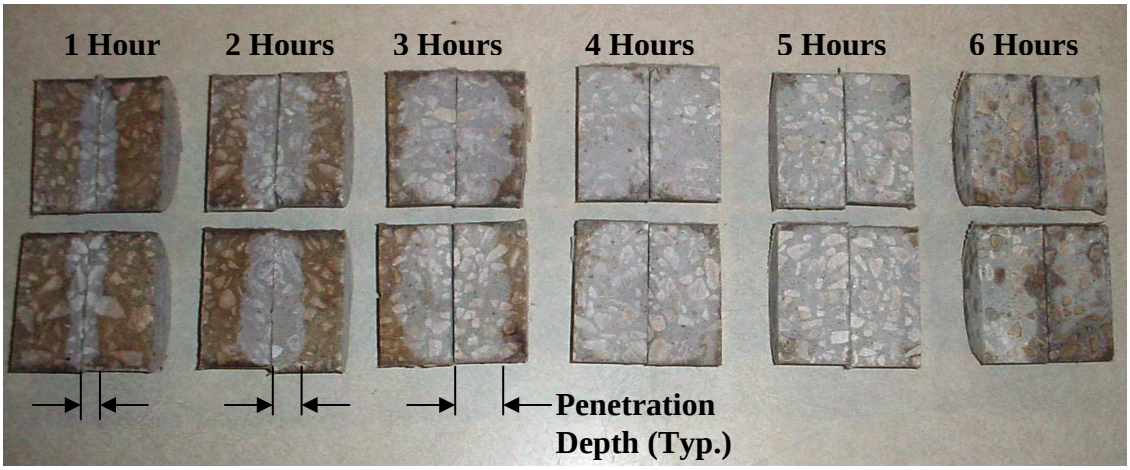

Figure 5-14: Chloride penetration depth on 2 split specimens from each hour of the RCPT

The above results are reported for Mix 11 after 7 days moist curing. This being a relatively porous mixture at 7 days of curing, the penetration depth extends entirely through the specimen after the fourth hour of testing. As seen in Figure 5-13 above, the values for current in the highly permeable specimens peak at approximately three hours into the test and steadily decrease thereafter until the end of the test. A possible explanation for the reduction in charge passed, which indicates reduced chloride ion flow is chloride binding. After a chloride ion becomes bound to the concrete matrix, it can no longer move. Only the chloride ions that are not bound can still move through the matrix. As some ions become bound, the free chloride concentration is therefore reduced, thereby increasing the resistance to movement of chloride ions. This phenomenon is discussed by Stanish (2004) in an explanation of chloride ion transport in concrete.

The results of the RCPT in this report were modified to exclude the increased current induced by heating of the specimens and solution. The total charge passed during the first 30 minutes was measured by finding the area under the curve of the current versus time plot for each specimen. The 30-minute Coulomb values were multiplied by 12 to provide values equivalent to a 6-hour test.

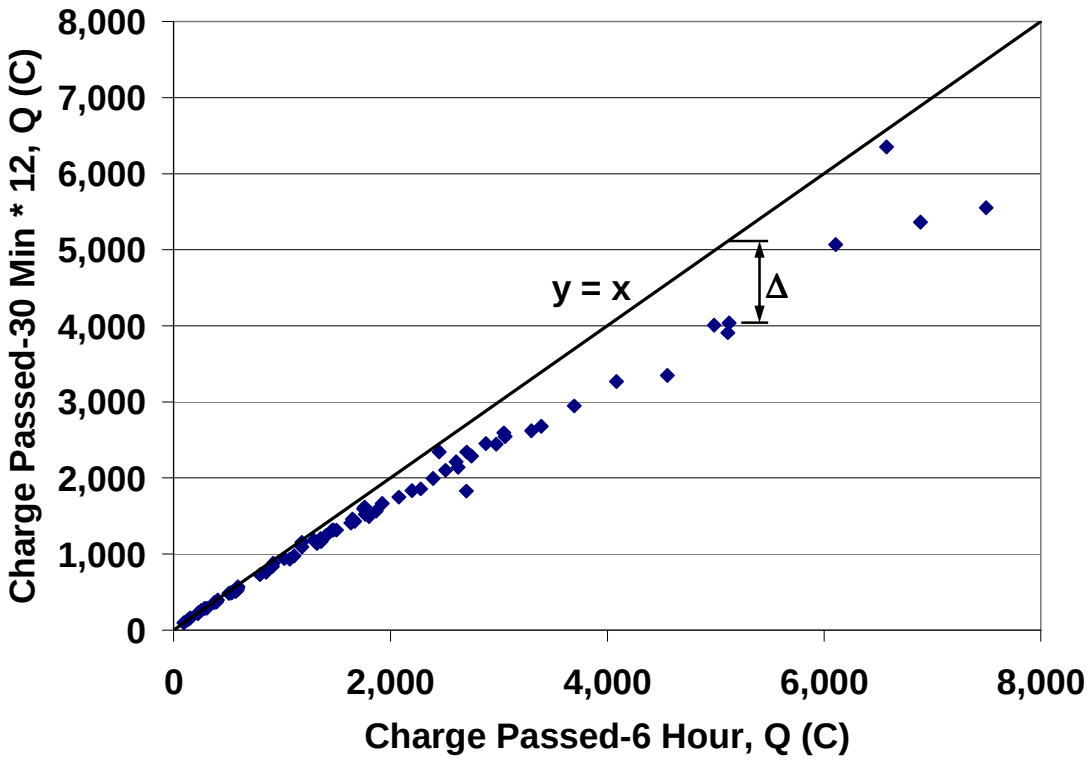

Figure 5-15: Comparison of charge passed values for 6-hour test and 30-minutes*12

Figure 5-15 compares values for total charge passed in the standard 6 hour RCPT on the x-axis to the values for charge passed for 30 minute RCPT multiplied by 12 on the y-axis. The plot includes results from all mixtures at 7, 28, and 56 days moist curing. As shown in Figure 5-15 the specimens having higher permeability have a larger difference (Δ) between the 6 hour and 30 minute values. This further highlights the observation that there is an increase in the 6-hour chloride permeability values, likely caused by heating in the specimens. The heating effect is more evident in the more permeable specimens. Chloride permeability values reported from this point forward are results of 30 minutes of testing multiplied by 12.

5.3.2 Effects of Water to Binder Ratio

The following plots illustrate the effects of water to binder ratio on the chloride penetration. The effects of cement composition can also be compared between 7, 28, and 56 days of moist curing by comparing the plots to each other.

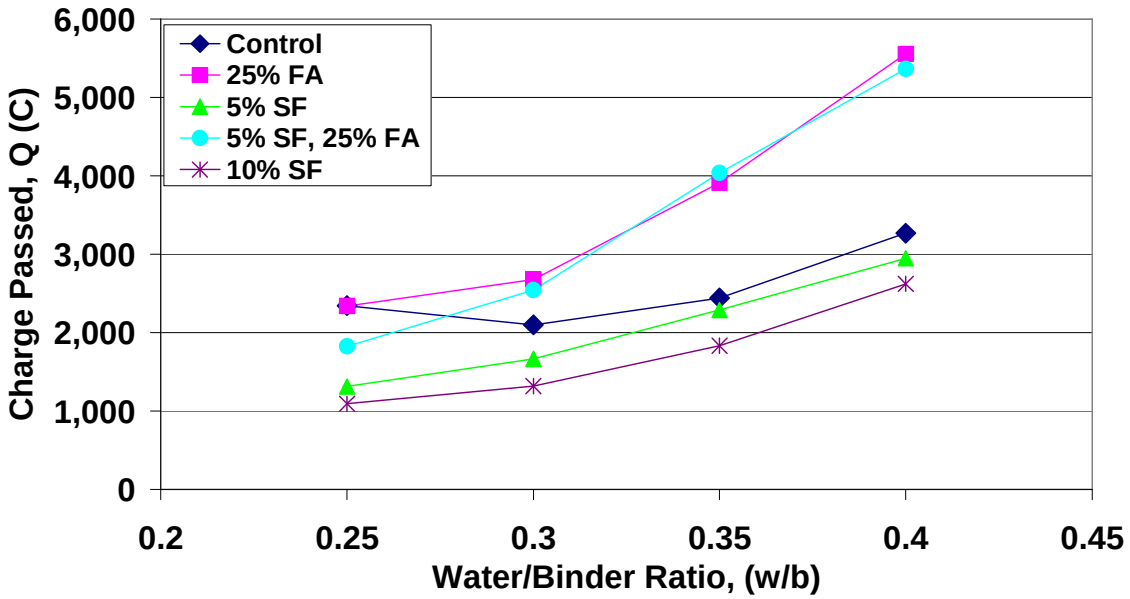

Figure 5-16: Influence of water to binder ratio on the RCPT total charge passed at 7 days moist cure

The results illustrated after 7 days of moist curing are generally not meaningful to the overall performance of concrete. However, by comparing the early age results to those at later ages, one can determine how characteristics such as strength and durability are enhanced with curing time. This can create a better understanding of the development of the concrete microstructure during the curing process.

Expected trends in the results do appear as early as 7 days of moist curing. One such obvious trend is increased chloride permeability as the water to binder ratio increased from 0.25 to 0.40. This increased water to binder ratio has a greater effect on the mixtures containing fly ash. It is also observed that the ternary mixture containing

25% fly ash and 5% silica fume has negligible differences in the chloride permeability results when compared to the binary mixture having only 25% fly ash. The reduction in chloride permeability by having 10% silica fume compared to 5% silica fume at this early age is very small as seen in Figure 5-16.

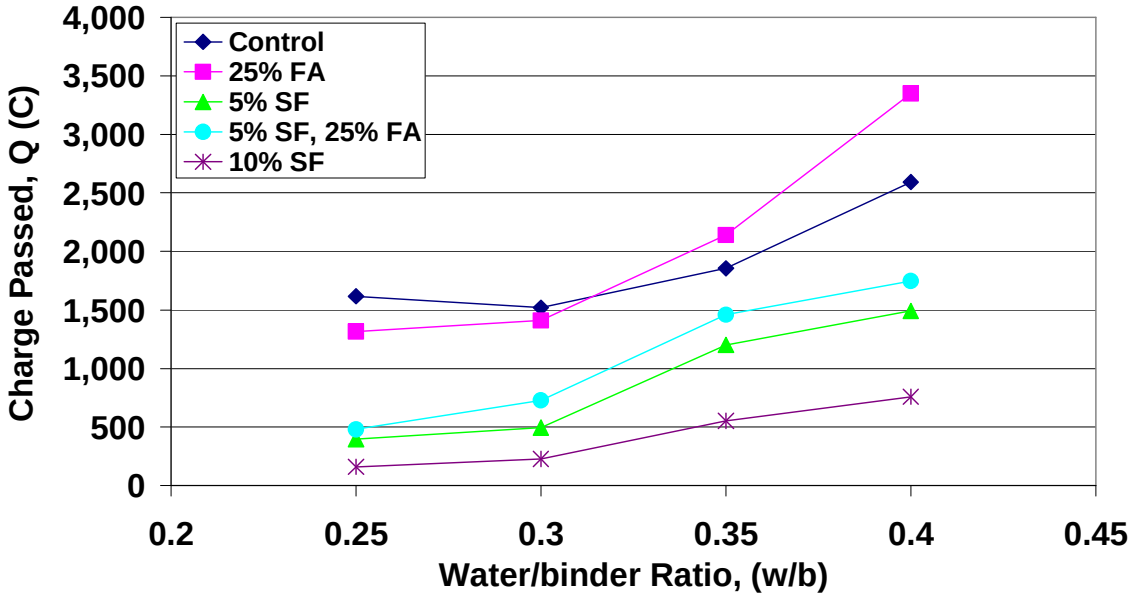

Figure 5-17: Influence of water to binder ratio on the RCPT total charge passed at 28 days moist cure

After 28 days of moist curing time, there is a distinct improvement in chloride permeability reduction in the 10% silica fume mixtures versus the 5% mixtures as shown by Figure 5-16 and Figure 5-17. The chloride penetration of the 10% SF mixtures is about half that of the 5% SF mixtures at all w/b ratios. However, nearly all values for both mixtures are in the "Very Low" range defined by ASTM C-1202. The benefit to cost ratio of the further reduction in chloride penetration produced by the 10% silica fume mixtures may or may not be advantageous at this point. The addition of 5% silica fume to the 25% fly ash mixture only produces a decrease in total charge passed of approximately 200 Coulombs. Also observed after 28 days is the negligible difference between the control mixture and the 25% fly ash mixtures at the low w/b ratios. In

addition, the chloride penetration value for the 0.40 w/b ratio control mixture is only about 700 Coulombs lower than the 25% fly ash mixture compared to nearly 2,000 Coulombs difference at 7 days.

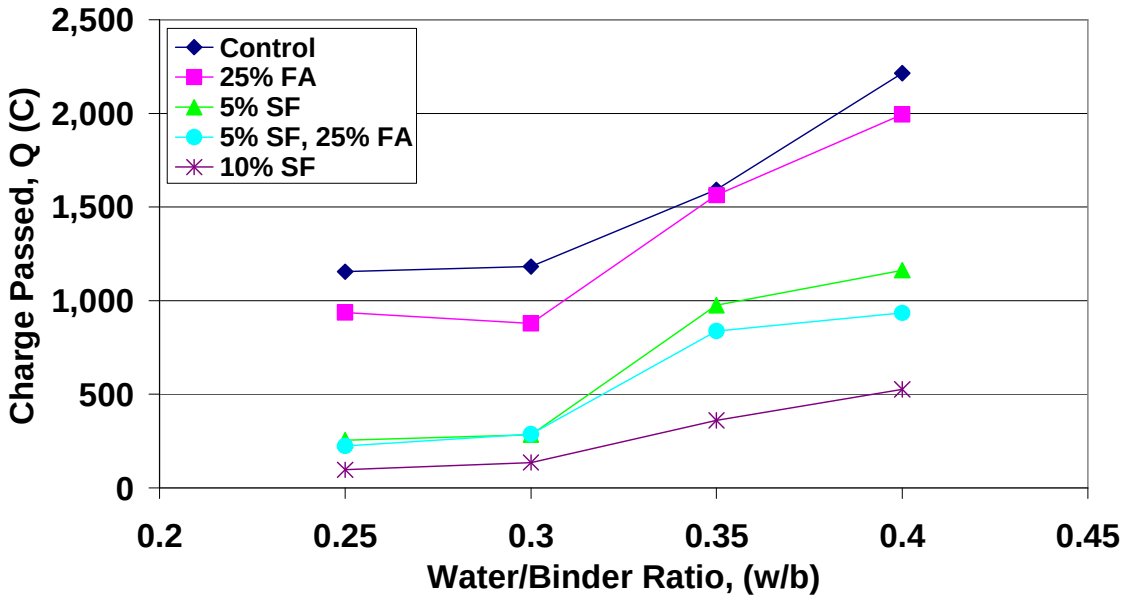

Figure 5-18: Influence of water to binder ratio on the RCPT total charge passed at 56 days moist cure

The results after 28 and 56 days of moist curing are similar when comparing the mixtures to each other. The chloride penetration values only continue to decrease between 28 and 56 days. Figure 5-18 indicates that the control mixture has negligible advantage over the 25% fly ash mixtures at all water to binder ratios with respect to chloride permeability reduction. Similarly, there is negligible decrease in chloride permeability values when comparing the 5% silica fume only mixture to the ternary blend. In both cases, increased water to binder ratio increases chloride permeability with a more noticeable increase between 0.3 and 0.35 w/b. The addition of 5% silica fume to the control and the 25% fly ash decreases the total charge passed by 500 to 1000 Coulombs. The 10% silica fume blended mixtures provide the lowest chloride permeability values. This is expected from the dense matrix provided by the silica fume

blends. The chloride permeability values from the 10% silica fume mixtures are in the "negligible" and "very low" ranges as defined in ASTM C-1202. While the use of 10% silica fume reduces the value for charge passed compared to using only 5% silica fume, the reduction in coulombs passed is approximately 100 Coulombs in the low water to binder ratio mixtures. The further reduction from the 5% silica fume mixtures having permeability values in the "very low" range defined by ASTM C-1202 can likely be sacrificed to create a more economic mixture.

5.3.3 Effects of Cement Composition in Ternary Blended Mixtures

The following plots display the effects of cement composition for the 9 mixtures tested from the 0.3 water to binder series. This series includes the 4 ternary blend mixtures tested. Mixtures were tested with 5 and 10% silica fume replacement, 25 and 50% fly ash replacement, and combinations of these cement replacement levels.

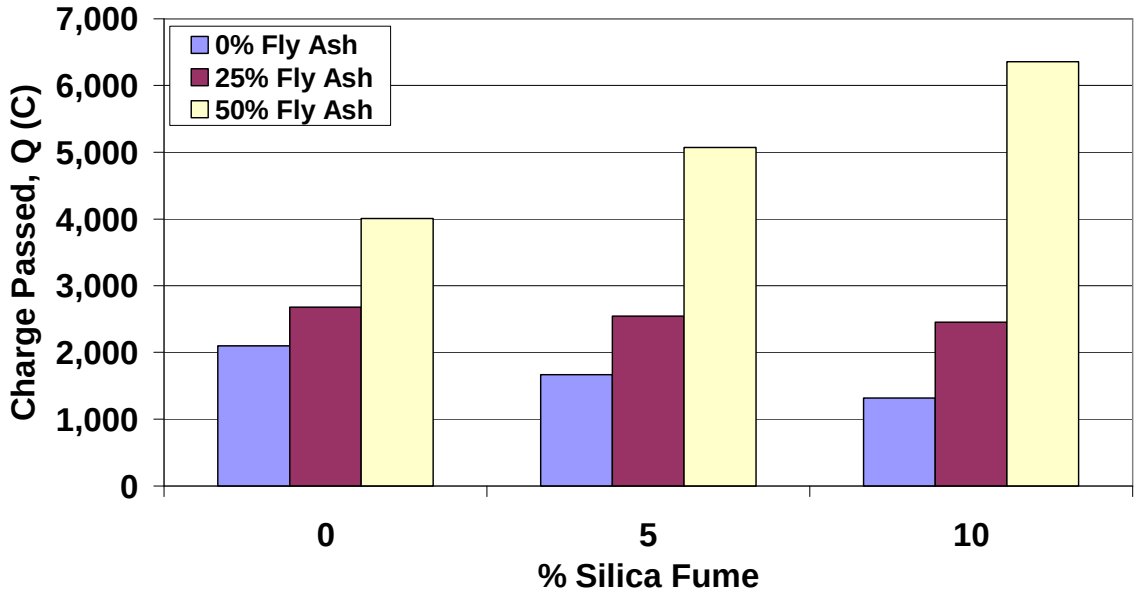

Figure 5-19: Influence of cement composition on the RCPT total charge passed at 7 days moist cure for 0.3 w/b mixes

As shown in Figure 5-19, the slow reacting properties of fly ash are evident by the increase in chloride permeability with the increase in fly ash replacement level. The chloride permeability increases with the amount of cement replaced by fly ash independent of silica fume replacement level. However, an unexpected result of increased permeability with the addition of silica fume in the 50% fly ash blends is present. The delayed reaction of the fly ash and therefore delayed pore structure development create highly permeable concrete after only 7 days of moist curing. The 50% fly ash appears to reduce the effect of the silica fume such that it has no effect at 7 days.

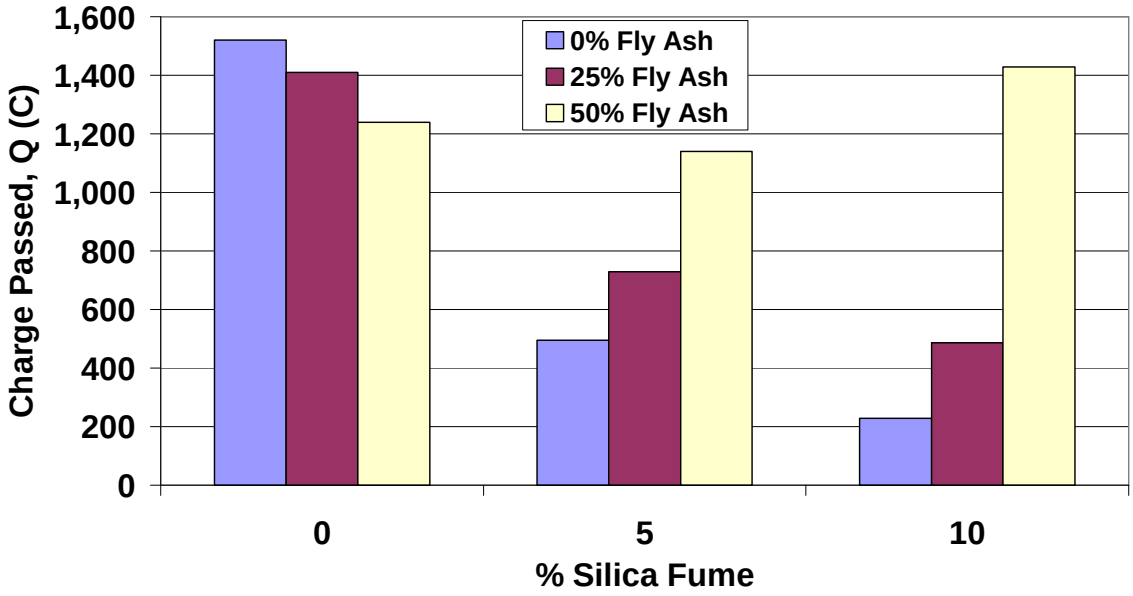

Figure 5-20: Influence of cement composition on the RCPT total charge passed at 28 days moist cure for 0.3 w/b mixes

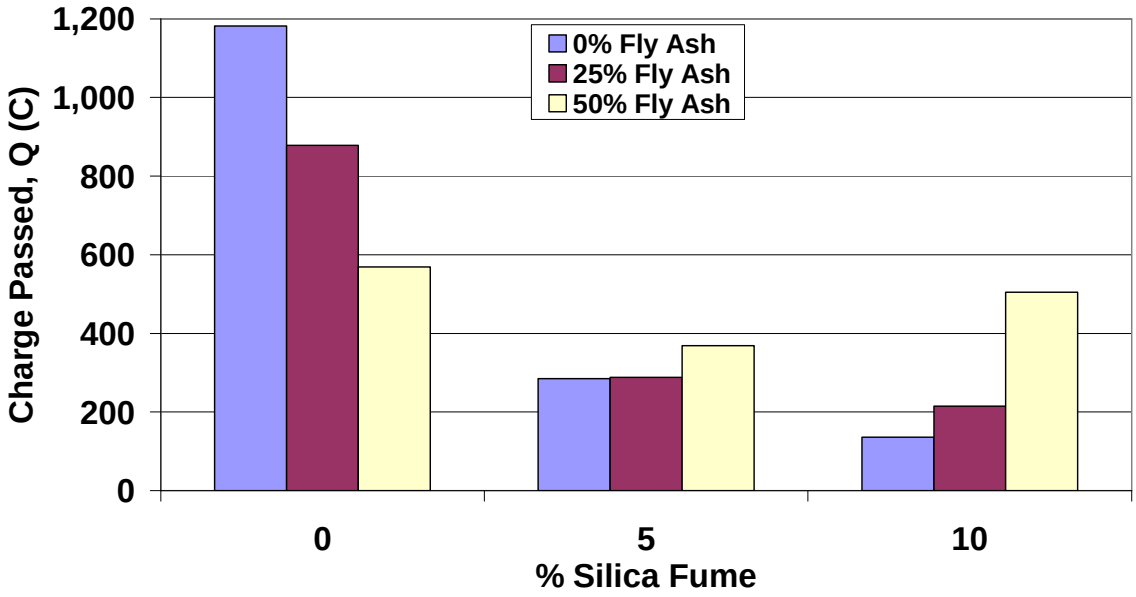

Figure 5-21: Influence of cement composition on the RCPT total charge passed at 56 days moist cure for 0.3 w/b mixes

The trends are very similar when comparing mixtures to each other at 28 and 56 days of moist curing. One unexpected result is the fact that at 28 and 56 days of moist curing, there seems to be an increase in chloride permeability with an increase in silica fume from 5% to 10% for the high volume fly ash mixtures. The addition of fly ash only reduces chloride permeability values by approximately 50% when increased from 0 to 50%. Likewise, the increase from 0 to 10 % silica fume produces a reduction in chloride permeability by nearly 90%. The ternary blends tend to create an effect that reduces silica fume's effectiveness in reducing chloride permeability though long term chloride permeability is still in the "very low" range with 50% fly ash mixtures. The 50% fly ash controls the pore structure development such that the silica fume does not reduce the chloride permeability as in mixtures with less fly ash replacement.

5.3.4 Effects of Curing Time

The RCPT was conducted after 7, 28, and 56 days of moist curing of the specimens. The plots below illustrate the reduction in chloride permeability as moist curing time increased. The mixtures are compared to each other at all four levels of w/b ratio.

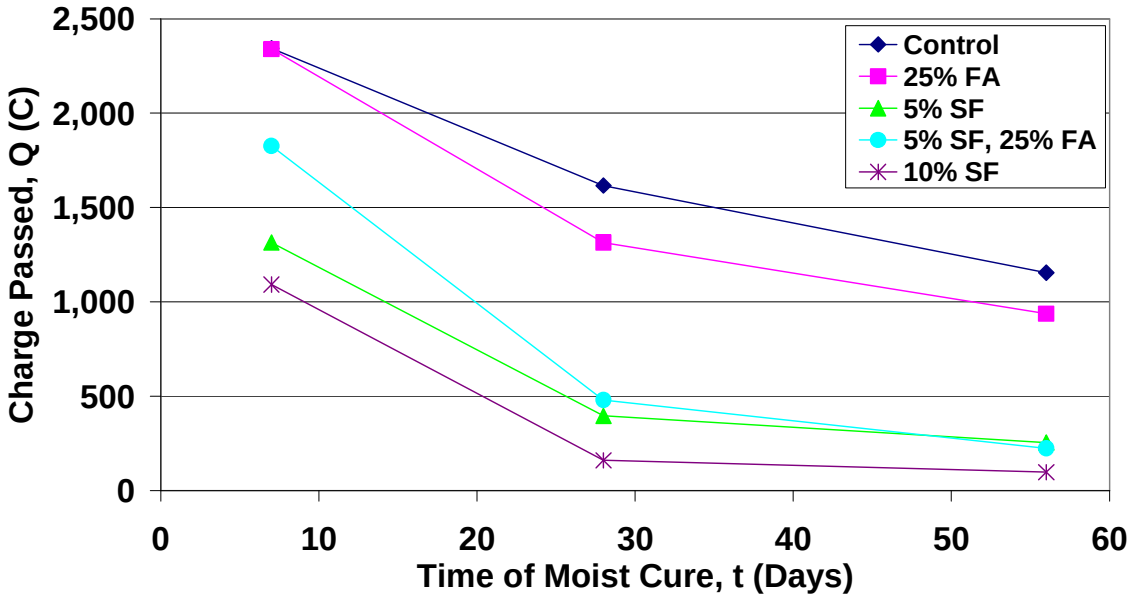

Figure 5-22: Influence of moist cure time on the RCPT total charge passed for 0.25 water to binder ratio concretes

A few observations can be made from Figure 5-22 for the 0.25 water to binder ratio mixtures. Among the 0.25 water to binder ratio mixtures, the largest reduction in chloride permeability is seen in those mixtures containing silica fume. The ternary mixture provided the largest decrease of approximately 1,800 Coulombs between 7 and 28 days of moist curing. All binary and ternary mixtures having the low 0.25 w/b ratio resulted in chloride penetration in the negligible or very low range after 56 days of moist curing. A difference of approximately 200 coulombs is seen between the 5 and 10%

silica fume mixtures at all curing times, indicating little benefit from the additional silica fume at the low water to binder level.

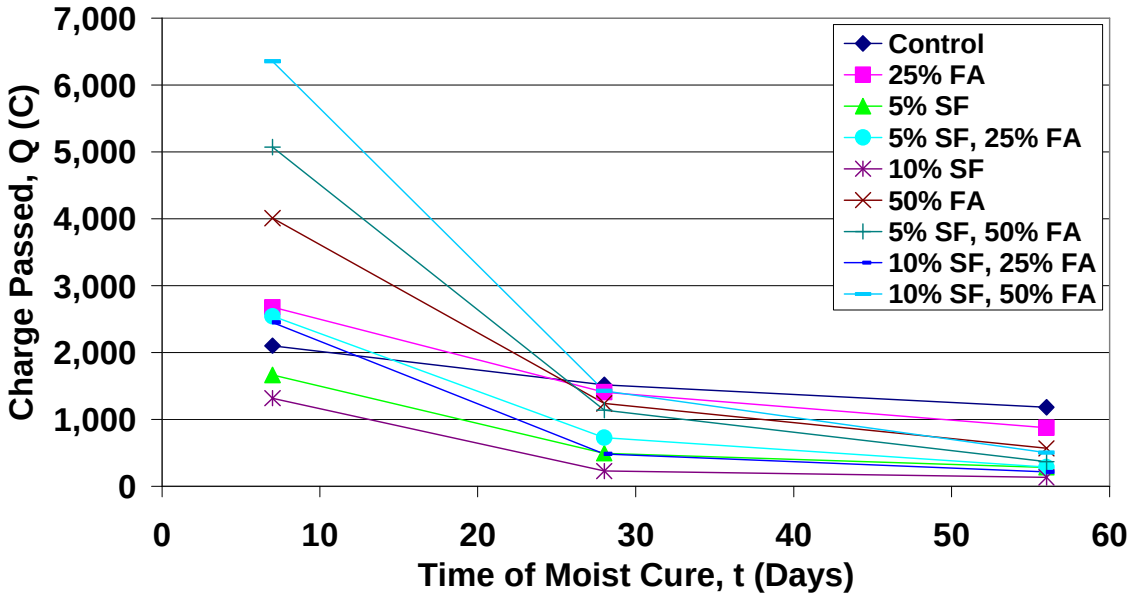

Figure 5-23: Influence of moist cure time on the RCPT total charge passed for 0.30 water to binder ratio concretes

In the mixtures containing 50% fly Ash, there was a 60 to 70 percent reduction in chloride penetration values from 7 to 28 days of curing time. These 50% fly ash mixtures had values in the "high" range at 7 days and were reduced to the "low" range after 28 days of moist curing. The reduction in chloride penetration was less prevalent in the mixtures having 25% or 0% fly ash. At 56 days of moist curing, all ternary blends have chloride permeability values in the range of 300 to 600 Coulombs passed. All mixtures except for the control provided 56 day results in the "very low" range. The control mixture was still in the "low" range with 1182 Coulombs passed.

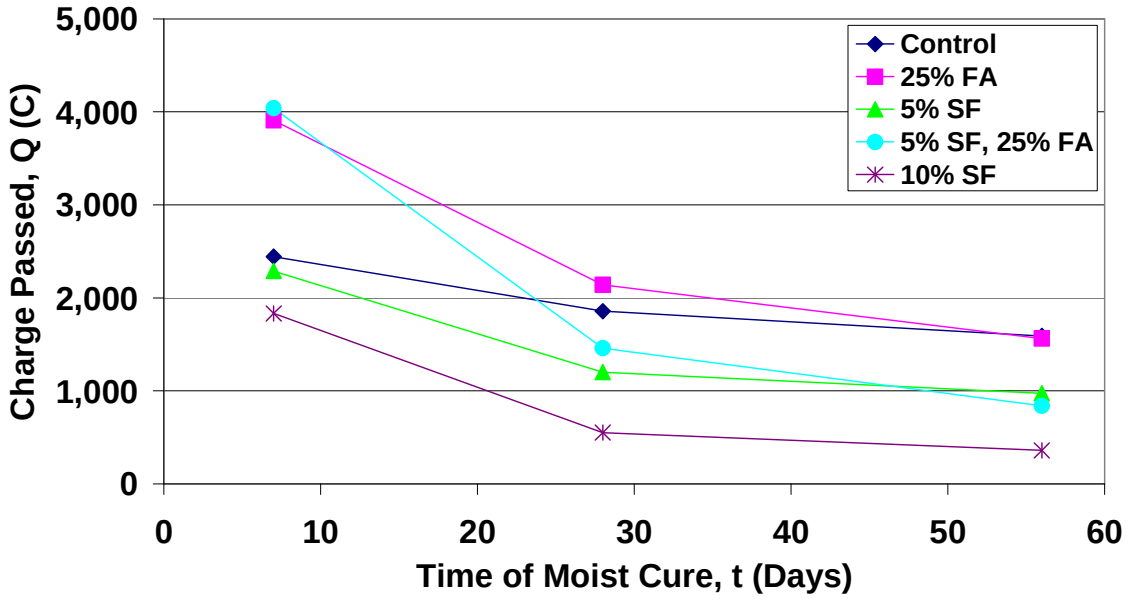

Figure 5-24: Influence of moist cure time on the RCPT total charge passed for 0.35 water to binder ratio concretes

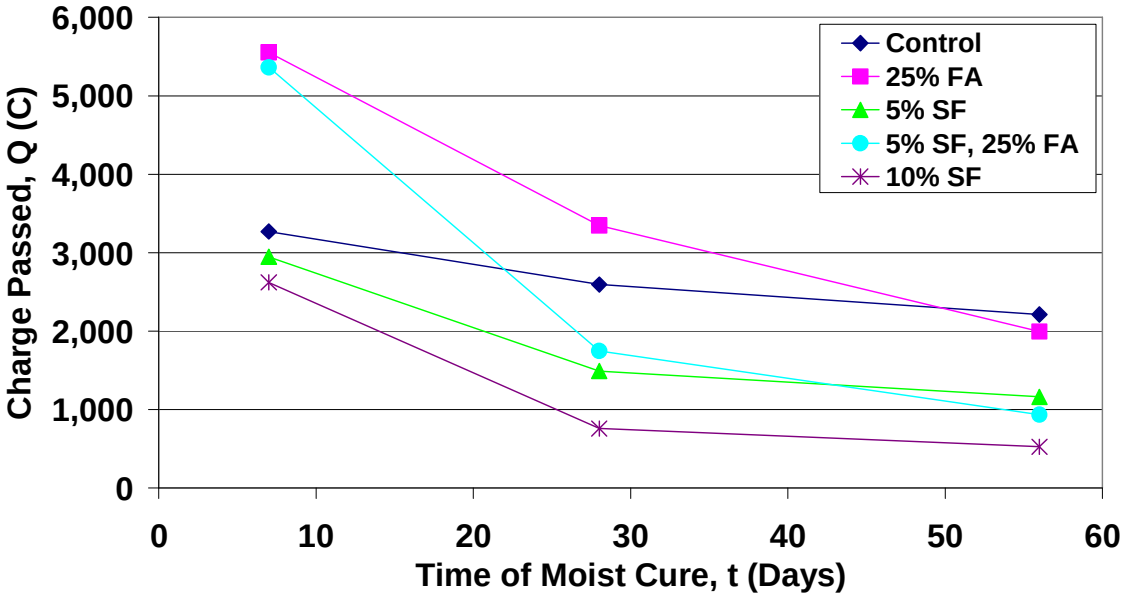

Figure 5-25: Influence of moist cure time on the RCPT total charge passed for 0.40 water to binder ratio concretes

As indicated by Figure 5-24 and Figure 5-25, the 0.35 and 0.40 water to binder ratio mixtures have very similar trends when comparing the results of mixtures to each other. The chloride permeability values of the 0.40 w/b mixtures ranged from 10 to 50% higher than their counterparts with 0.35 w/b ratio. The similar trends seem to appear for

all water to binder series as shown in Figure 5-22 through Figure 5-25. The chloride permeability values for similar mixtures are only higher as the water to binder ratio increases. It is evident at all water to binder ratios that moist curing time has the largest effect on mixtures containing fly ash.

The difference between 5 and 10% silica fume is parallel at all w/b levels. The separation between them tends to increase with the w/b ratio. The additional 5% silica fume in the 10% mixtures is less effective at the lower water to binder ratios.

Fly ash only and the control mixture reduce steadily from 7 through 56 days, but the addition of silica fume produces a greater reduction in the time between 7 and 28 days. The long term results of the 25% fly ash and the control mixtures are similar. This would indicate that fly ash can be used as a cement replacement to create a more economical mixture, provided other concrete qualities are also similar or improved by the use of fly ash. It is also evident from the figures above that the addition of fly ash, silica fume, or both is beneficial in reducing chloride penetration. The 56 day values for the control mixture were the highest for all water to binder levels tested.

Long term chloride permeability results were reported by (Bleszynski et al. 2002). Tests were conducted on binary mixtures containing silica fume or ground granulated blast furnace slag and ternary mixtures containing varying amounts of both. The slag generally exhibits durability properties similar to fly ash, having a delayed reaction time. In this study the ternary mixtures had chloride permeability values lower than the binary mixtures. The tests were conducted at 90 days, 1 year, and 2 years. This is similar to the permeability of the ternary mixture in the above results having continually decreasing values. Only the 10% silica fume mixture had lower permeability values than the ternary

mixture at 56 days curing. As seen in Figure 2-5 of this report, the ternary mixtures have lower values than the 8% Silica Fume mixture only after the 90 day tests.

(Nassif and Suksawang 2002) reported results for a mixture having 5% silica fume and 10% fly ash at varying water to cement ratios and curing times. Coulomb values were in the same range of the values for 5% silica fume and 5% silica fume and 25% fly ash ternary blends reported above. The results are also similar in that curing time has less effect on reduction of chloride permeability for lower w/b ratios.

5.4 Freeze-Thaw

Freeze-thaw tests were conducted according to ASTM C-666 for each of the 24 mixtures. Two specimens from each mixture were tested and the results were averaged. The following table lists the freeze-thaw test results by their durability factor along with the descriptions of each mixture.

Table 5.2: Freeze-thaw results listed by mixture

Mix #	w/b Ratio	Silica Fume Content (%)	Fly Ash Content (%)	Air Content (%)	Durability Factor
1	0.25	0	0	4.0	95.8
2	0.25	0	25	4.7	93.6
3	0.25	5	0	4.0	96.2
4	0.25	5	25	5.3	95.9
5	0.25	10	0	4.2	90.7
6	0.3	0	0	5.5	98.4
7	0.3	0	25	6.0	96.7
8	0.3	0	50	6.8	95.9
9	0.3	5	0	5.1	96.2
10	0.3	5	25	6.1	95.7
11	0.3	5	50	7.5	95.9
12	0.3	10	0	4.5	93.7
13	0.3	10	25	4.5	98.2
14	0.3	10	50	7.0	87.7
15	0.35	0	0	4.5	92.5
16	0.35	0	25	5.6	98.2
17	0.35	5	0	6.0	91.6
18	0.35	5	25	7.5	95.5
19	0.35	10	0	5.7	93.4
20	0.4	0	0	5.2	96.9
21	0.4	0	25	4.5	97.4
22	0.4	5	0	7.5	94.5
23	0.4	5	25	4.2	96.2
24	0.4	10	0	10.0	90.7

As seen in Table 5.2, the air contents of the fresh concrete mixtures varied from 4 to 7.5% with one exception. Mix 21 (0.40 w/b ratio with 10% silica fume) had an air content of 10%.

5.4.1 Effects of Water to Binder Ratio

The results of the freeze-thaw tests are plotted versus number of cycles in Appendix B. Figures B-1 through B-5 separates the results of each of the cement composition series. Each plot includes the results of each of the four w/b ratios. A definite trend does not appear in these plots for the affect of water to binder ratio on the freeze-thaw durability. The relative dynamic modulus of elasticity ranged between 0.92 and 0.98 for nearly all mixtures.

5.4.2 Effects of Cement Composition

Figures B-6 through B-9 in Appendix B display durability factor versus number of cycles for each of the different cement compositions. The plots are separated for each w/b ratio. The effects of cement composition are not apparent by these results after 300 freeze-thaw cycles.

All mixtures resulted in durability factors greater than 90 except for Mix 14. This mixture had cement replacement with 10% silica fume and 50% fly ash and a resulting durability factor of 87.7. The lower durability factor may be expected in the mixtures containing 50% fly ash. The freeze-thaw specimens were placed into the chamber at 28 days. The pore structure of the high volume fly ash concrete was likely still developing at 28 days of curing according to the chloride permeability and compressive strength results. At this time, the hydration process was likely halted due to the freezing of the specimens.

The range of the relative dynamic modulus of elasticity for the mixes is within approximately 10%. It could be argued that this is easily within acceptable error of the ASTM C-666 and ASTM C-215 tests. The fundamental transverse frequency of the

specimens was measured according to ASTM C-215, which lists a single operator margin of error of 2%. When comparing mixtures to other there is a possibility of 4% error, more than half the difference in durability factor between all mixtures.

CHAPTER 6 CONCLUSIONS

6.1 Summary

This project involved a comprehensive study of high performance concrete durability with respect to its resistance to chloride permeability and freeze-thaw damage. The project concentrated on studying the effects of binary and ternary blended cements containing silica fume and/or fly ash, along with varying water to binder ratio and curing time, on the pore structure of HPC. A full understanding of the pore structure provides the ability to engineer high performance concrete mixtures for durability. The results of this study can be combined with the results from the overall project, which includes time-dependent properties such as creep and shrinkage, to optimize HPC blends for uses in bridge applications.

6.2 Conclusions

Conclusions drawn from the chloride permeability, freeze-thaw, and compressive strength test components of this experimental program are listed below.

6.2.1 Chloride Penetration

This study comprehensively looks at the effects of w/b ratio, cement composition and curing time on the chloride permeability of 24 different concrete mixtures.

The RCPT results were modified to include only the first 30 minutes of the test. This excluded increased current and resulting increased values for total charge passed caused by heating in the relatively high permeable mixtures. The values for the 30 minutes of testing were converted to values equivalent to the standard 6-hour test by

simply multiplying them by 12. A look at the time current responses of the specimens in this study indicates that the mixtures most affected by heating from the "Joule Effect" are those tested at 7 days of curing. The mixtures containing fly ash appear the most affected. While results from 7 days of curing are useful in understanding pore structure development, results from 28 and 56 days are more useful as they serve as standard reference times for compressive strength tests on concrete cylinders with and without fly ash, respectively.

Binary and ternary mixtures containing 25% fly ash provides chloride permeability resistance at 56 days similar to control mixtures without fly ash. There would likely be continued reduction in permeability beyond 56 days of curing provided by continued reaction of the fly ash. The cost of fly ash being approximately one fourth that of Portland cement provides cost saving benefit that does not reduce the quality of the concrete with regard to durability. Fly ash use is also more environmentally friendly than the use of Portland cement.

The 50% fly ash replacement also provides resistance to chloride permeability that is superior to the control mixture and the 25% fly ash binary mixture. The high volume (50%) fly ash mixture provides chloride permeability that is approximately one-half that of the control mixture. This advantage is not evident, however, until after 28 days of curing time. High volume fly ash mixtures can provide adequate durability provided the pore structure is allowed enough time to develop prior to chloride exposure.

The efficiency of silica fume replacement tends to decrease with lower w/b ratios. At the lower w/b ratios tested, 0.25 and 0.30, there is negligible advantage with regard to chloride penetration of having 10% silica fume over 5% silica fume. It is likely that

additional water is not available for the reaction of more than 5% silica fume at the low water to binder levels.

The direct effects of water to binder ratio on durability are relatively better known. Lower w/b ratio concretes have a finer pore structure and are therefore more resistant to chloride permeability. This effect is also readily noticeable in the results presented in this report. However, water to binder ratio had different effects depending on the cement composition. Higher chloride permeability values caused by increasing the w/b ratio were reduced in mixtures with silica fume replacement of cement. Low water to binder ratios ($\leq$0.30) resulted in all binary and ternary blended mixtures with chloride permeabilty values in the "very low" range at 56 days of curing.

6.2.2 Freeze-Thaw Durability

Results from the freeze-thaw testing completed during this project were very similar to those found in published literature (ACI Committee 201 2001), (Cramer 2001), and (Ozyildirim 1987). There were no clearly identifiable trends to compare the mixtures to each other given the very limited change in durability factor and experimental scatter typical with testing concrete mixtures. The tests proved that properly air entrained concrete is generally resistant to the effects of freeze-thaw cycles provided the air content is equal to at least 4%.

6.2.3 Compressive Strength

The compressive strength results from this study generally follow trends that are accepted from available literature. The increased porosity and less dense microstructure that results from higher water to binder ratios were evident among all mixtures.

Compressive strengths were reduced with increased water to binder ratio in nearly all cases as would be expected.

The 56 day results for the ternary blends indicate that the addition of silica fume has a relatively small effect on increasing compressive strength. In mixtures containing fly ash, the addition of silica fume resulted in compressive strength increases that were less than 10%. The lower compressive strengths seen in the fly ash mixtures at 7 days are an indication of the longer reaction time of fly ash and its delayed pore structure development.

The effect of curing time on high volume fly ash concrete tends to be different for compressive strength and chloride permeability. The compressive strength values continue a steady increase from 7 to 56 days of curing. The chloride permeability decrease between 7 and 28 days is much more dramatic than between 28 and 56 days of curing. Development of the concrete microstructure with curing is evident among all mix types.

LIST OF REFERENCES

AASHTO T 259. (2001). *Standard method of test for resistance of concrete to chloride ion penetration*, American Association of State Highway and Transportation Officials.

AASHTO T 260. (2001). *Standard method of Test for Sampling and Testing for Chloride Ion in Concrete and Concrete Raw Materials*, American Association of State Highway and Transportation Officials.

AASHTO TP 64-03. (2003). *Standard Method of Test for Predicting Chloride Penetration of Hydraulic Cement Concrete by the Rapid Migration Procedure*, American Association of State Highway and Transportation Officials.

ACI Committee 201. (2001). *Guide to durable concrete*, American Concrete Institute, Detroit, Mich.

ACI Committee 232. (1996). *Use of fly ash in concrete*, American Concrete Institute, Farmington Hills, MI.

American Society for Testing And Materials. (1997a). *ASTM C 666 - 97: Standard test method for resistance of concrete to rapid freezing and thawing*, Astm, Philadelphia, PA.

American Society for Testing And Materials. (1997b). *ASTM C 1202 - 97: Standard test method for electrical indication of concrete's ability to resist chloride ion penetration*, Astm, Philadelphia, PA.

American Society for Testing And Materials. (2001). *ASTM C 138-01: Standard Test Method for Density (Unit Weight), Yield, and Air Content (Gravimetric) of Concrete*, Astm, Philadelphia, PA.

American Society for Testing And Materials. (2003a). *ASTM C 143-03: Standard Test Method for Slump of Hydraulic-Cement Concrete*, Astm, Philadelphia, PA.

American Society for Testing And Materials. (2003b). *ASTM C 231-03: Standard Test Method for Air Content of Freshly Mixed Concrete by the Pressure Method*, Astm, Philadelphia, PA.

Babu, K. G. a. K., V. Sree Rama. "Chloride Diffrusivity of GGBFS Concretes." *Fly Ash, Silica Fume, Slag and Natural Pozzolans in Concrete, SP-1199*, Chennai (Madras), India, 611-620.

Bleszynski, R. F., Hooton, R. D., Thomas, M. D. A., and Rogers, C. A. (2002). "Investigations into the Durability of Ternary Blend Concrete: Laboratory and Outdoor Exposure Site Studies." TRB 2002 Annual Meeting CD-Rom, Federal Highway Administration, Washington, D.C.

Blomberg, J. M. (2003). "Laboratory Testing of Bridge Deck mixes." *RDT 03-004*, Missouri Department of Transportation Research, Development, and Technology.

Cabrera, J. G., and Claisse, P. A. (1990). "Measurement of chloride penetration into silica fume concrete." *Cement & Concrete Composites*, 12(3), 157-161.

Chia, K. S., and Zhang, M.-H. (2002). "Water permeability and chloride penetrability of high-strength lightweight aggregate concrete." *Cement & Concrete Research*, 32(4 April), 639-645.

Cohen, M. D., Zhou, Y., and Dolch, W. L. (1992). "Non-air-entrained high-strength concrete - Is it frost resistant?" *ACI Materials Journal*, 89(4 Jul-Aug), 406-415.

Cramer, S. M. "Mix Parameters Controlling the Extended Freeze-Thaw durability of Concrete containing Cementitious Additives." *Proceedings: 81st Transportation Research Board Conference, Papers CD-Rom*, Washington D.C.

Ghosh, S., and Nasser, K. W. (1995). "Creep, shrinkage, frost, and sulphate resistance of high strength concrete." *Canadian Journal of Civil Engineering*, 22(3n), 621-636.

Gopalaratnam, V. S., Earney, T. P., and Stundebeck, C. J. "High Performance Concrete for Bridge Applications -- Issues Related to Durability and Time Dependant Response." *Advances in Cement and Concrete*, Copper Mountain, Colorado, 303-313.

Hooton, R. D. (1986). "Permeability and Pore Structure of Cement Pastes Containing Fly Ash, Slag, and Silica Fume." *ASTM Special Technical Publication 897. Publ by ASTM, Philadelphia, PA, USA*, 128-143.

Hooton, R. D. (1993). "Influence of silica fume replacement of cement on physical properties and resistance to sulfate attack, freezing and thawing, and alkali-silica reactivity." *ACI Materials Journal*, 90(2 Mar-Apr), 143-151.

Julio-Betancourt, G. A. a. H., R. D. (2004). "Study of the Joule effect on rapid chloride permeability values and evaluation of related electrical properties of concretes." *Cement & Concrete Research*, 34, 1007-1015.

Kashi, M. G., and Weyers, R. E. "Freezing and thawing durability of high strength silica fume concrete." *Proc Sess Relat Struct Mater Struct Congr. Publ by ASCE, New York, NY, USA. 89*, 138-148.

Luther, M. D., and Mikols, W. J. "Ternary and Quaternary Concrete Mixtures Containing GGBF Slag." *Use of Fly Ash, Silica Fume, Slag, and Other By-Products in Concrete and Construction Materials*, Milwaukee, WI.

Malhotra, V. M. (1990). "Durability of concrete incorporating high-volume of low-calcium (ASTM Class F) fly ash." *Cement & Concrete Composites*, 12(4), 271-277.

Mokhtarzadeh, A. (1995). "Mechanical properties and durability of high-strength concrete for prestressed bridge girders." Transportation research record. No. 1478, 20-29.

Nassif, H., and Suksawang, N. "Effect of Curing Method on Durability of High Performance Concrete." *TRB Anual Meeting CD-ROM*, Washington, DC.

Oh, B. H., Cha, S. W., Jang, B. S., and Jang, S. Y. (2002). "Development of high-performance concrete having high resistance to chloride penetration." *Nuclear Engineering & Design*, 212(1-3 March), 221-231.

Ozyildirim, C. (1987). "Laboratory Investigation of Concrete Containing Silica Fume for Use in Overlays." *ACI Materials Journal*, 84(1), 3-7.

Plante, P., and Bilodeau, A. (1989). "Rapid Chloride Permeability Test: Data on Concrete Incorporating Supplementary Cementing Materials." Fly Ash, Silica Fume, Slag and Natural Pozzolans in Concrete, V. M. Malhotra, ed., American Concrete Institute, Trondheim, Norway, 626-644.

Sabir, B. B. (1997). "Mechanical properties and frost resistance of silica fume concrete." *Cement & Concrete Composites*, 19(4 Aug), 285-294.

Stanish, K., Hooton, R.D., and Thomas, M.D.A. (2004). "A novel method for describing chloride ion transport due to an electrical gradient in concrete: Part 1. Theoretical description." *Cement and Concrete Research*, 34, 43-49.

Stanish, K. D., Hooton, R. D., and Thomas, M. D. A. (1997). "Testing the Chloride Penetration Resitance of Concrete: A Literature Review."

Tang, L., and Nilsson, L.-O. (1997). "Rapid determination of the chloride diffusivity in concrete by applying an electrical field." *ACI Materials Journal*, 89(1), 40-53.

Zia, P., and Hansen, M. R. (1993). "Durability of high performance concrete." Pacific Rim TransTech Conference, ASCE, New York, NY, 398-404.

Zia, P., Leming, M. L., Ahmad, S. H., and Program, C. A. S. H. R. (1991). *High performance concretes : a state-of-the-art report*, Strategic Highway Research Program National Research Council, Washington, D.C.

APPENDIX A CHLORIDE PERMEABILITY DATA

Table A.1: 7 Day Chloride Permeability Data - 6 Hour Test

	Chloride Permeability Charge Passed, Q (C)						
	Specimen 1			Specimen 2			
Mix #	Top	Middle	Bottom	Top	Middle	Bottom	Overall Average[1]
1	2801	2729	2844	2723	2846	2783	2450
2	3110	3133	3123	---	2996	3065	2704
3	1738	1780	1615	---	1610	1627	1463
4	3151	3193	2972	---	3021	3053	2699
5	1358	1393	1336	1345	1304	1348	1184
6	2727	2823	2744	3016	2907	2904	2508
7	4053	3920	3572	4468	3614	3517	3390
8	5585	5743	5367	5757	5959	5630	4986
9	2235	2226	2231	2117	2204	2134	1926
10	3631	3384	3471	3419	3491	3484	3059
11	---	6774	6891	7202	6805	7181	6106
12	1703	1779	1657	1673	1677	1569	1473
13	---	3346	3167	3397	3343	3156	2881
14	7625	7603	7078	7690	7491	7415	6577
15	3407	3270	3507	3513	3457	3158	2975
16	6083	5363	5702	5942	6048	5756	5112
17	3169	3266	3262	3029	3047	2993	2749
18	6153	5969	5681	6379	5880	4906	5122
19	2790	2429	2248	2522	2600	2413	2198
20	4659	4866	4447	4899	4929	4089	4085
21	10345	8409	7580	8579	9205	7052	7496
22	4344	4452	3701	4273	4574	3884	3695
23	6975	7996	8753	7886	8452	6974	6890
24	3787	3856	3761	3758	4007	3365	3301

[1] Average adjusted for 4" Specimen, Value multiplied by $(3.75/4.00)^2$

Table A.2: 28 Day Chloride Permeability Data - 6 Hour Test

	Chloride Permeability Charge Passed, Q (C)						
	Specimen 1			Specimen 2			
Mix #	Top	Middle	Bottom	Top	Middle	Bottom	Overall Average[1]
1	1967	2044	2171	2043	1954	1847	1762
2	1749	1729	1731	1724	1734	1577	1501
3	502	510	456	434	426	440	406
4	608	609	603	544	546	569	510
5	160	215	203	175	140	158	154
6	2045	2079	1925	2011	1979	2013	1765
7	1860	1940	1790	1808	1890	1863	1634
8	1603	1703	1411	1628	1709	1537	1405
9	595	564	571	607	655	638	532
10	908	915	886	857	954	913	796
11	1544	1375	1376	1533	1607	1589	1322
12	262	283	292	253	216	252	228
13	600	579	604	565	650	643	533
14	2006	1904	1898	1777	1916	1913	1672
15	2597	2637	2544	2507	2614	2660	2279
16	3211	2918	2722	3158	3146	2771	2626
17	1550	1557	1549	1552	1575	1465	1355
18	1927	1847	1854	1957	1917	1752	1649
19	716	702	647	728	631	609	591
20	3664	3474	3284	3593	3521	3248	3045
21	5371	4873	5297	5233	5166	5150	4554
22	2140	2070	2020	2151	2043	1878	1802
23	2361	2378	2174	2570	2363	2341	2078
24	1029	970	950	981	964	935	854

[1] Average adjusted for 4" Specimen, Value multiplied by $(3.75/4.00)^2$

Table A.3: 56 Day Chloride Permeability Data - 6 Hour Test

	Chloride Permeability Charge Passed, Q (C)						
	Specimen 1			Specimen 2			
Mix #	Top	Middle	Bottom	Top	Middle	Bottom	Overall Average[1]
1	1261	1340	1418	1398	1460	1208	1184
2	1050	1266	1192	1232	1133	1099	1021
3	296	330	318	258	270	251	252
4	252	278	243	284	263	230	227
5	97	112	119	101	109	106	94
6	1454	1523	1442	1477	1553	1394	1295
7	978	1081	1117	1034	1061	1004	919
8	719	717	615	733	654	603	592
9	247	306	364	341	383	303	285
10	354	378	340	334	347	335	306
11	441	435	463	477	443	439	395
12	142	182	136	136	148	162	133
13	256	216	288	252	246	261	222
14	620	641	591	693	677	675	571
15	2082	2000	1750	2086	2160	1887	1753
16	2116	2255	1990	2154	2221	2022	1869
17	1215	1282	1251	1348	1266	1223	1111
18	1089	1004	1041	1019	1142	935	913
19	415	440	421	465	456	371	376
20	2955	3278	2661	3152	3066	2681	2606
21	2651	2821	2738	2900	2519	2712	2394
22	1615	1616	1359	1670	1582	1454	1362
23	1318	1151	1150	1195	1253	1236	1070
24	638	619	661	696	746	644	586

[1] Average adjusted for 4" Specimen, Value multiplied by $(3.75/4.00)^2$

Table A.4: 7 Day Chloride Permeability Data - 30 Min x 12 Test

	Chloride Permeability Charge Passed, Q (C)						
	Specimen 1			Specimen 2			
Mix #	Top	Middle	Bottom	Top	Middle	Bottom	Overall Average x 12[1]
1	230	220	217	213	218	235	2344
2	219	222	232	---	219	219	2339
3	126	133	125	---	122	121	1314
4	185	221	209	---	209	215	2200
5	103	110	103	103	101	103	1092
6	190	193	195	210	204	203	2100
7	268	260	246	265	243	243	2679
8	375	382	361	386	398	379	4009
9	164	164	157	149	160	154	1666
10	251	233	241	236	245	242	2544
11	---	475	473	500	467	497	5070
12	127	130	122	125	125	121	1317
13	---	241	229	235	234	222	2453
14	597	625	565	623	617	589	6354
15	235	227	241	239	228	220	2443
16	386	353	365	374	376	370	3909
17	220	222	223	212	212	212	2288
18	409	389	373	405	392	330	4038
19	191	171	163	173	180	165	1833
20	327	334	304	279	331	284	3269
21	596	518	501	538	544	463	5555
22	291	289	252	284	294	267	2948
23	469	519	557	512	541	455	5364
24	248	254	248	251	265	225	2621

[1] Average adjusted for 4" Specimen, Value multiplied by $(3.75/4.00)^2$

Table A.5: 28 Day Chloride Permeability Data - 30 Min x 12 Test

	Chloride Permeability Charge Passed, Q (C)						
	Specimen 1			Specimen 2			
Mix #	Top	Middle	Bottom	Top	Middle	Bottom	Overall Average x 12[1]
1	155	155	170	151	146	143	1616
2	125	126	126	128	125	119	1315
3	40	40	38	36	36	36	397
4	47	47	47	44	44	45	480
5	14	18	18	16	11	15	161
6	146	148	138	143	142	147	1520
7	134	140	127	130	137	135	1410
8	114	123	105	121	129	113	1240
9	46	43	44	48	52	50	495
10	67	72	68	65	73	70	728
11	112	100	100	110	112	114	1139
12	22	23	24	22	18	22	228
13	43	44	46	43	50	50	486
14	142	134	136	131	133	137	1428
15	180	179	171	172	176	179	1856
16	220	203	180	210	210	195	2140
17	114	114	114	113	113	115	1201
18	143	137	135	142	141	132	1460
19	55	54	52	58	49	47	553
20	259	242	236	254	246	239	2593
21	325	311	319	320	315	316	3349
22	145	145	140	148	141	131	1492
23	165	164	157	179	163	165	1748
24	75	71	71	74	71	70	759

[1] Average adjusted for 4" Specimen, Value multiplied by $(3.75/4.00)^2$

Table A.6: 56 Day Chloride Permeability Data - 30 Min x 12 Test

	Chloride Permeability Charge Passed, Q (C)						
	Specimen 1			Specimen 2			
Mix #	Top	Middle	Bottom	Top	Middle	Bottom	Overall Average x 12[1]
1	99	106	117	114	118	102	1155
2	80	96	90	95	87	85	938
3	24	27	27	23	23	22	255
4	20	22	22	25	22	18	225
5	7	9	11	10	9	10	97
6	111	116	112	111	118	106	1182
7	77	87	89	82	84	81	879
8	56	56	51	59	52	50	569
9	21	26	29	29	32	26	285
10	27	29	28	27	27	26	288
11	33	35	36	38	35	34	369
12	11	15	12	12	12	16	136
13	20	18	23	20	20	21	215
14	44	47	45	50	50	51	505
15	155	153	138	157	159	144	1592
16	149	155	140	146	154	145	1563
17	88	94	94	97	91	91	976
18	86	77	78	79	85	73	838
19	31	35	35	39	36	29	361
20	216	225	191	222	211	195	2214
21	187	193	188	197	177	192	1994
22	114	115	98	116	112	106	1163
23	93	86	84	88	91	90	934
24	48	47	50	51	55	48	526

[1] Average adjusted for 4" Specimen, Value multiplied by $(3.75/4.00)^2$

APPENDIX B FREEZE-THAW DATA AND RESULTS

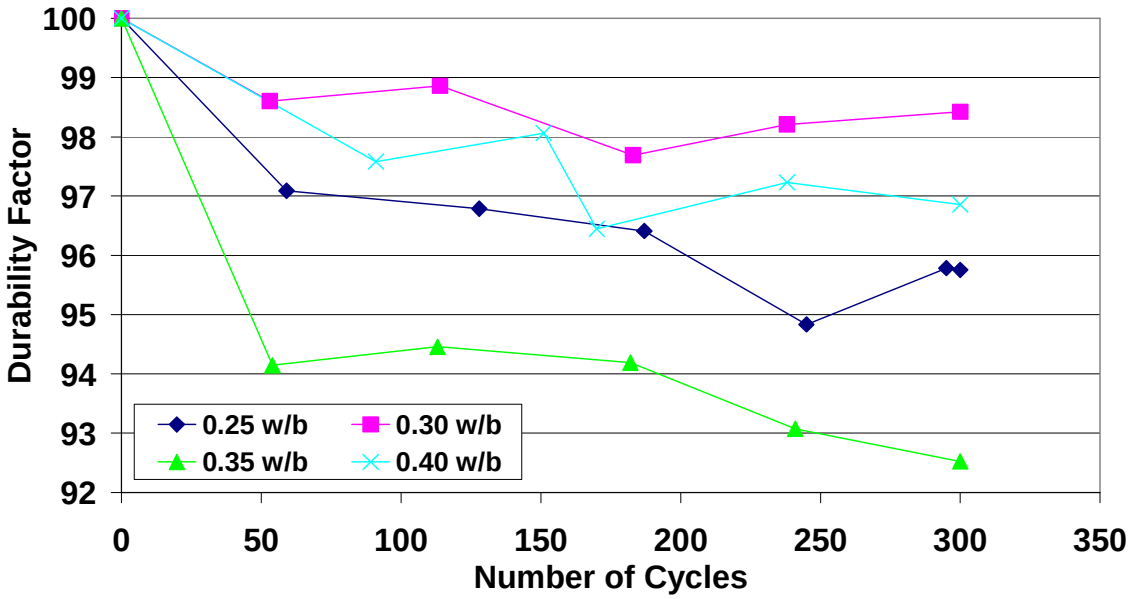

Figure B-1: Influence of w/b ratio on freeze-thaw durability factor for Control mixtures

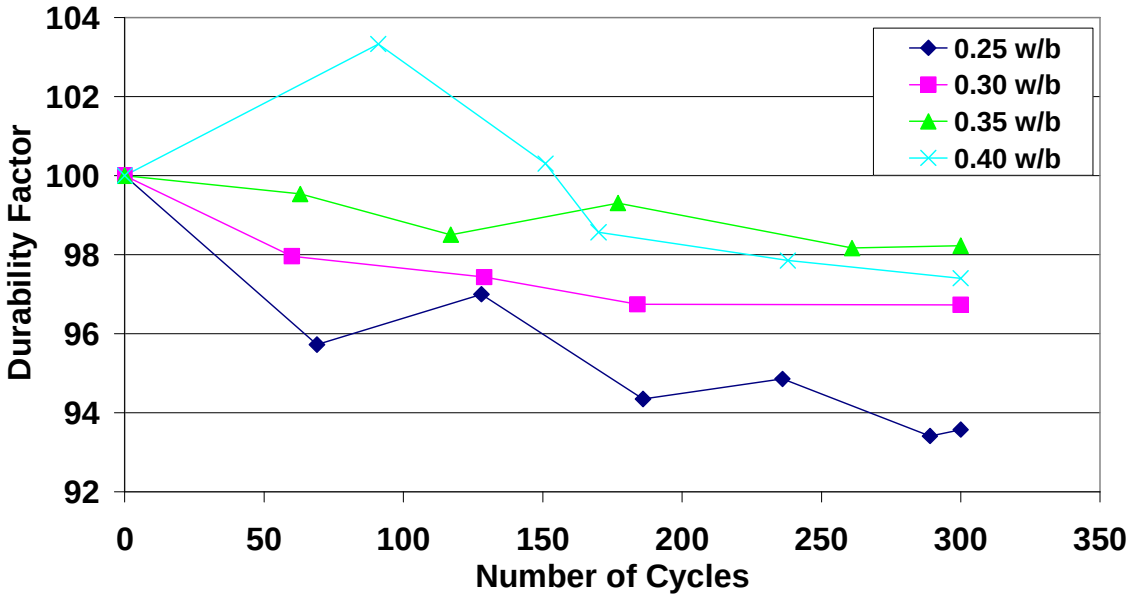

Figure B-2: Influence of w/b ratio on freeze-thaw durability factor for 25% fly ash mixtures

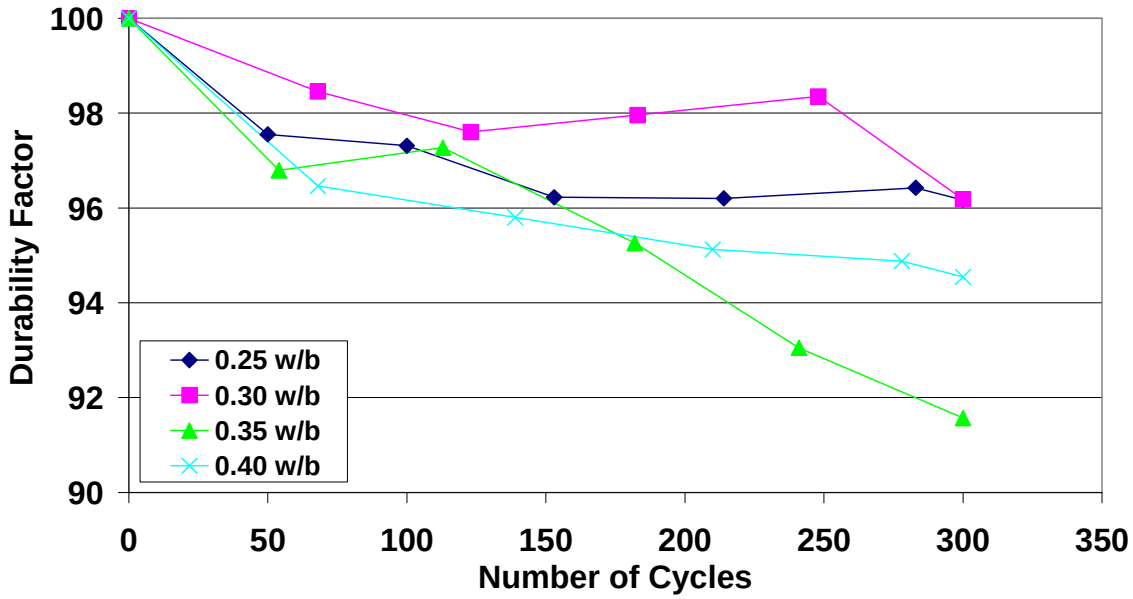

Figure B-3: Influence of w/b ratio on freeze-thaw durability factor for 5% silica fume mixtures

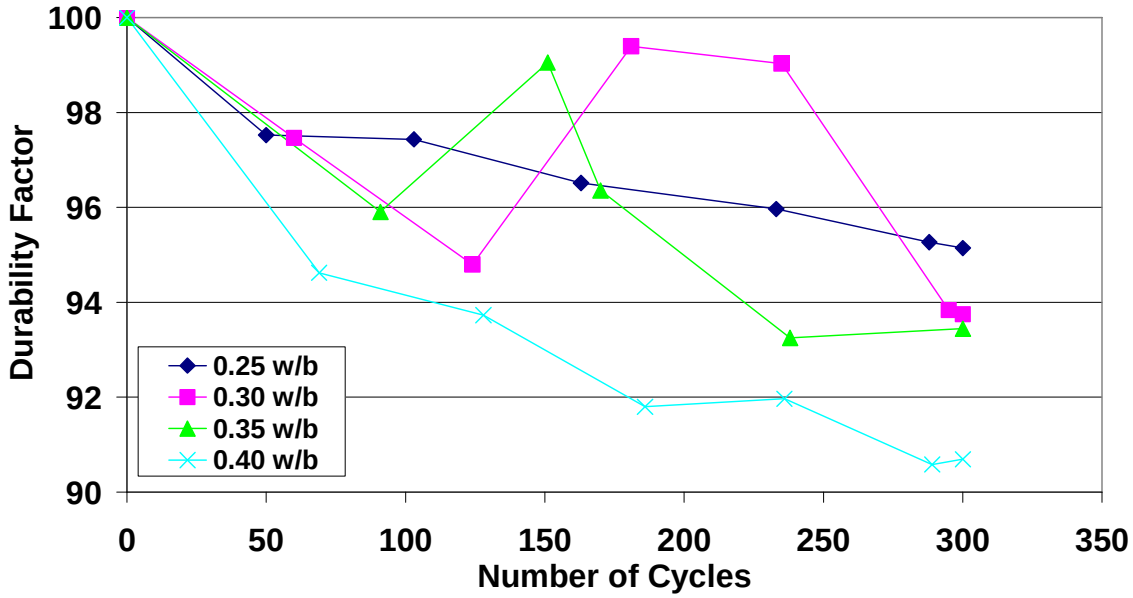

Figure B-4: Influence of w/b ratio on freeze-thaw durability factor for 10% silica fume mixtures

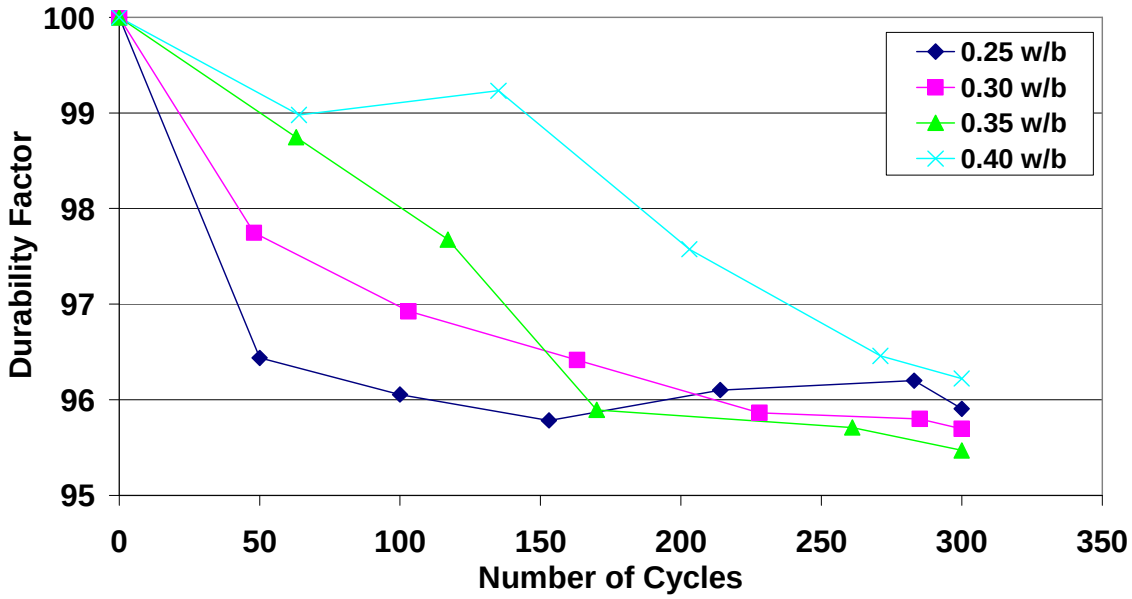

Figure B-5: Influence of w/b ratio on freeze-thaw durability factor for 5% silica fume and 25% fly ash ternary mixtures

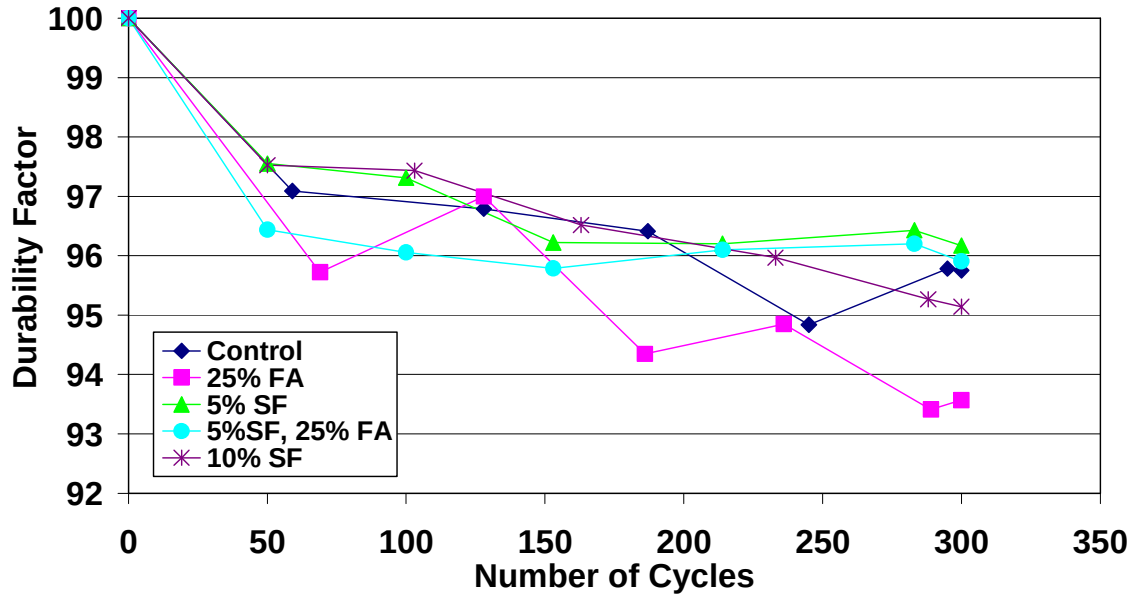

Figure B-6: Influence of cement composition on freeze-thaw durability factor for 0.25 w/b ratio mixtures

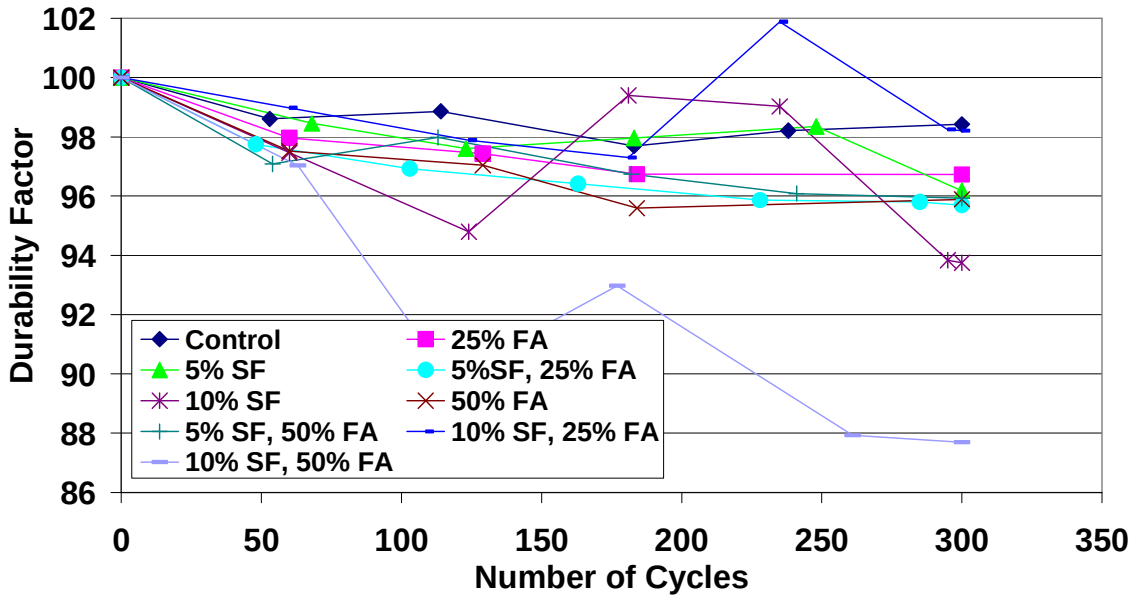

Figure B-7: Influence of cement composition on freeze-thaw durability factor for 0.30 w/b ratio mixtures

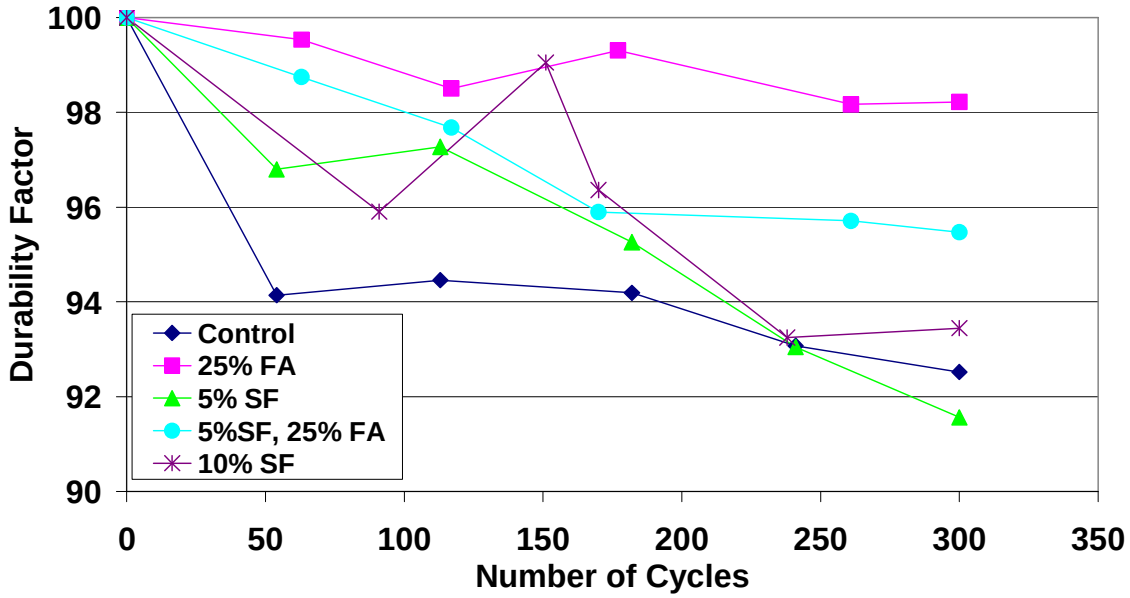

Figure B-8: Influence of cement composition on freeze-thaw durability factor for 0.35 w/b ratio mixtures

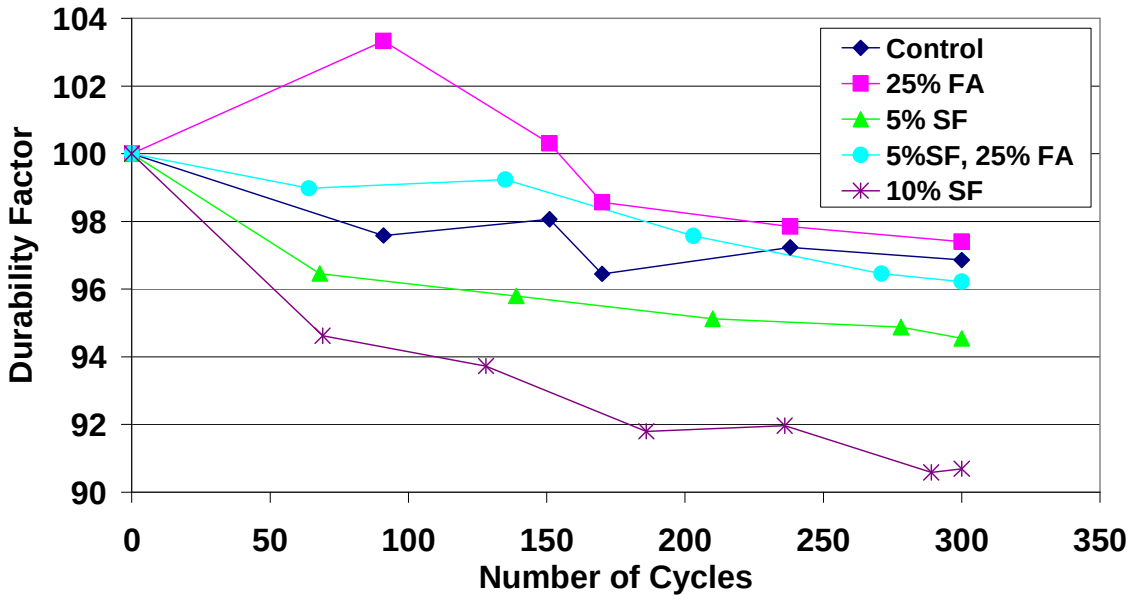

Figure B-9: Influence of cement composition on freeze-thaw durability factor for 0.40 w/b ratio mixtures

APPENDIX C COMPRESSIVE STRENGTH DATA

Table C.1: 7 Day Compressive Strength Data

	Compressive Strength, f'_c (psi)		
Mix #	Specimen 1	Specimen 2	Average
1	6836	7480	7158
2	7589	8699	8144
3	5741	6211	5976
4	7692	7263	7478
5	9253	9473	9363
6	8078	7832	7955
7	7286	6988	7137
8	6286	7082	6684
9	8329	8189	8259
10	6629	7971	7300
11	5758	5456	5607
12	9068	8502	8785
13	8067	7976	8022
14	5934	6310	6122
15	6700	6953	6827
16	5593	5555	5574
17	6733	5970	6352
18	4763	4794	4779
19	7420	7159	7290
20	4831	4821	4826
21	6097	5961	6029
22	4967	4378	4673
23	8918	8975	8947
24	4824	4688	4756

Table C.2: 28 Day Compressive Strength Data

	Compressive Strength, f'_c (psi)		
Mix #	Specimen 1	Specimen 2	Average
1	7272	7374	7323
2	9168	9232	9200
3	10409	9004	9707
4	8705	8628	8667
5	10575	9369	9972
6	8178	8023	8101
7	7635	7283	7459
8	7265	7746	7506
9	8285	8928	8607
10	8734	8611	8673
11	6631	6516	6574
12	8759	8618	8689
13	9282	8466	8874
14	8112	8775	8444
15	7560	7188	7374
16	6990	6558	6774
17	6892	7025	6959
18	6161	5802	5982
19	8204	8458	8331
20	6038	5888	5963
21	7208	6950	7079
22	5779	5719	5749
23	7873	6859	7366
24	4628	5093	4861

Table C.3: 56 Day Compressive Strength Data

	Compressive Strength, f'_c (psi)		
Mix #	Specimen 1	Specimen 2	Average
1	8106	5850	8106
2	9337	9248	9293
3	9844	9748	9796
4	8628	8236	8432
5	9829	10666	10248
6	8973	8386	8680
7	8164	8385	8275
8	8055	9006	8531
9	9140	8983	9062
10	7938	8967	8453
11	7809	7082	7446
12	10172	9581	9877
13	9002	9021	9012
14	8636	7964	8300
15	7777	7448	7613
16	7733	7336	7535
17	7721	8125	7923
18	6324	6115	6220
19	7861	8416	8139
20	6626	5967	6297
21	7216	7106	7161
22	5469	5915	5692
23	8068	8346	8207
24	6268	6025	6147

APPENDIX D FLY ASH LAB TEST RESULTS

ANALYTICAL TESTING SERVICE LABORATORIES, INC.
P.O. BOX 1118, JOPLIN, MISSOURI 64802
(417) 782-6573

Mineral Resource Tech. LLC
2700 Research Forest Drive
The Woodlands, Texas 77381-4226
1-281-362-1060

June 19, 2003

Attn: Mr. Jim Hicks

Re: 4247 - Labadie Silo D Fly Ash Sample - 3000 Ton Composite - 04/24-05/06/03

	AASHTO-M295-93 Class "C" Requirements	ASTM C-618 Class "C" Requirements	Actual
Fineness (+325 Mesh)	34% Max	34% Max	13.50%
Moisture Content	3% Max	3% Max	0.22%
Specific Gravity	****	****	2.73
Loss on Ignition	5% Max	6% Max	0.36%
Soundness	0.8% Max	0.8% Max	-0.01%
S.A.I., 7 Days	60% Min	75% Min	91.00%
S.A.I., 28 Days	****	75% Min	99.40%
Water Req. % Control	100% Max	105% Max	93.40%
Silica SiO_2	****	****	33.08%
Aluminum Oxide Al_2O_3	****	****	22.76%
Ferric Oxide Fe_2O_3	****	****	6.29%
Total	50% Min	50% Min	62.13%
Sulfur Trioxide SO_3	5% Max	5.0% Max	2.27%
Calcium Oxide CaO	40% Max	****	24.99%
Magnesium Oxide MgO	5% Max*	****	5.06%
Available Alkalies Na_2O	1.5% Max	****	1.50%

*The 5% Max limit can be exceeded if the autoclave expansion is within the allowable limit of 0.8%.

We certify the above was tested in accordance with ASTM C-618.

Analytical Testing Service Laboratories, Inc.

John K. Cupp, Manager

FROM : FAX NO. : Jul. 07 2003 09:08PM P2

Figure D-1: Fly ash lab test results sheet

APPENDIX E CHLORIDE PERMEABILITY TEST SETUP

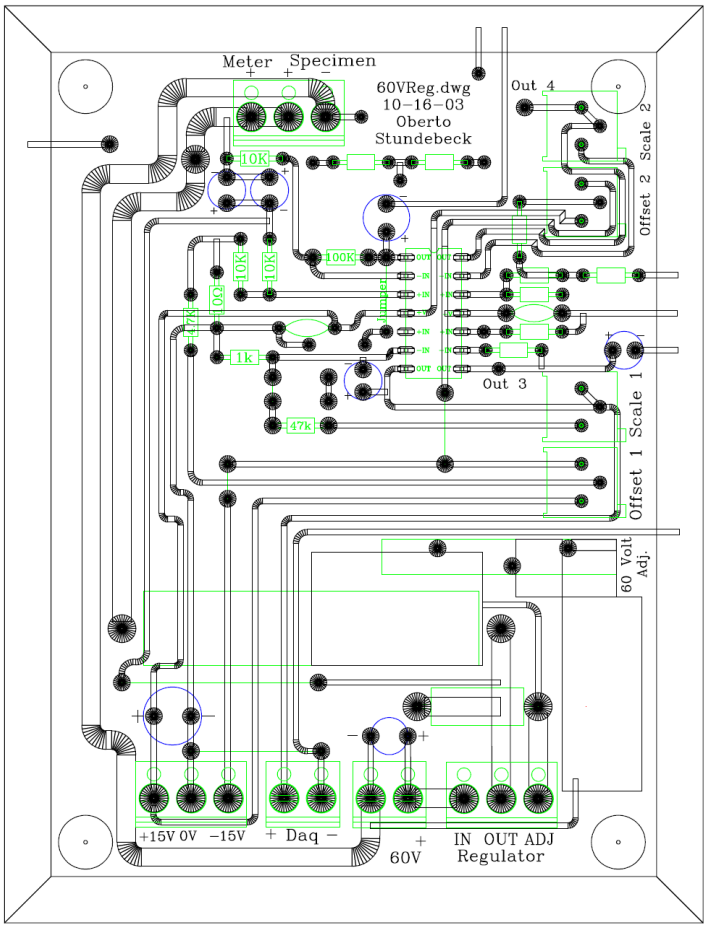

Figure E-1: AutoCAD Drawing of circuit board used for 60 V regulator and current measurement in Rapid Chloride Permeability Test

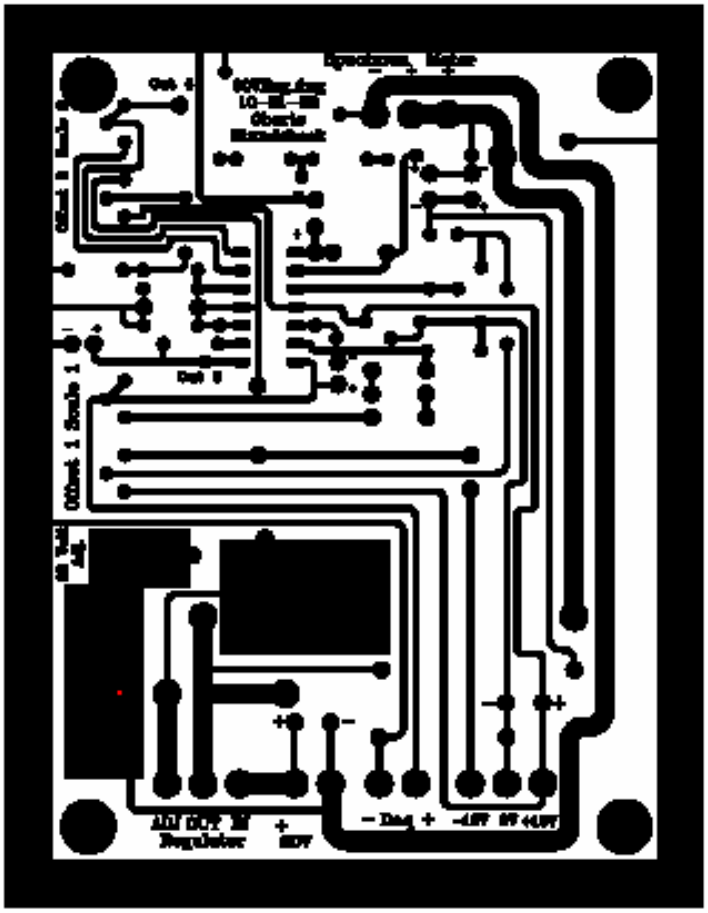

Figure E-2: Mirrored image used to make circuit boards used for 60 V regulator and current measurement in Rapid Chloride Permeability Test

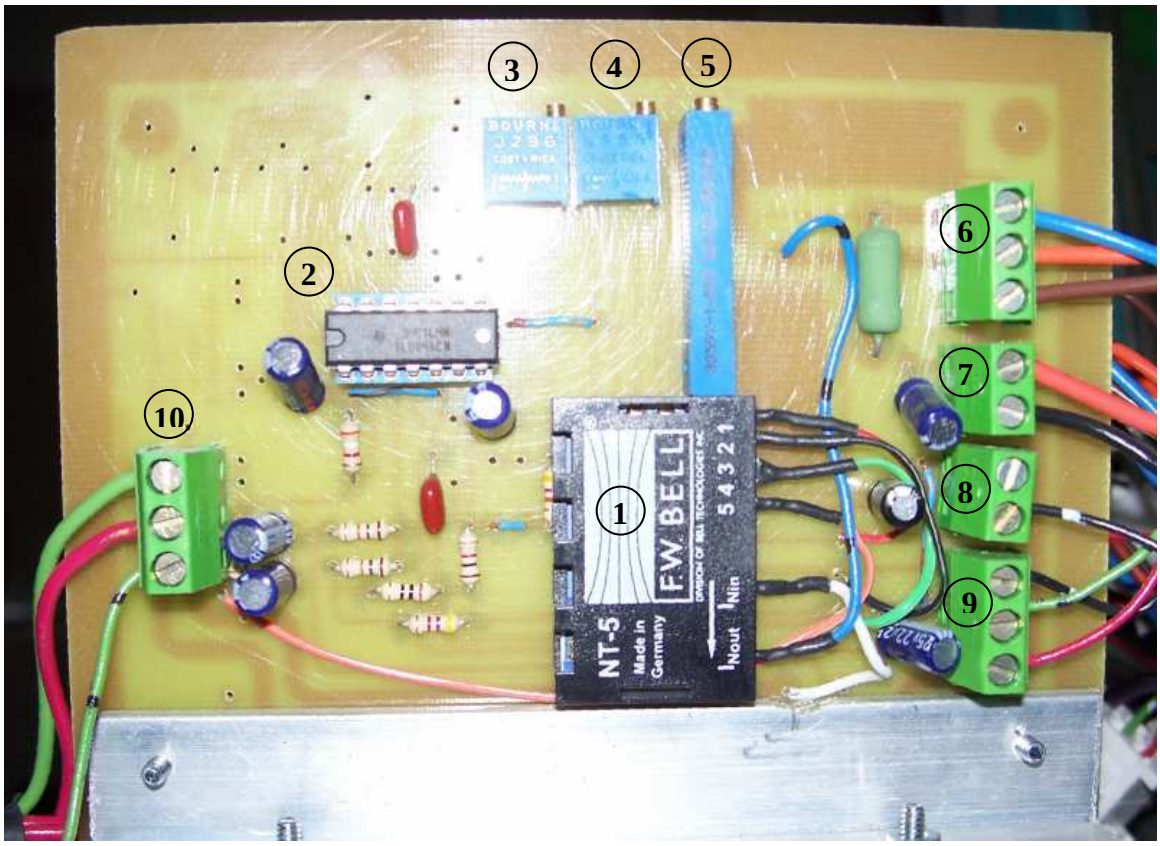

Figure E-3: 60 Volt Regulator and Current Measurement Circuit Board for Rapid Chloride Permeability Test

Figure E-3 Key

1. F.W. Bell NT-5 Isolated current measuring device.
2. TL084CN Quad Op-Amp for Data acquisition signal
3. Potentiometer for scale adjustment of current measurement
4. Potentiometer for offset adjustment of current measurement
5. Potentiometer for scale adjustment of ±60 V
6. Terminals to ±60 V Regulator
7. Terminals to unregulated ±60 V
8. Terminals to Data acquisition system and current display on front panel
9. Terminals to ±15 V Power Supply
10. Terminals for ±60 V to the specimens and voltage meter on front panel